...-80048/N Scientific and Technial Reports Summary (Cont'd)
Block 10 PREPARATION INSTRUCTIONS (Con't)

UNCLASSIFIED
SECURITY CLASSIFICATION OF THIS PAGE

AD-A261 690

REPORT DOCU

Form Approve
OMB No. 0704

1a. REPORT SECURITY CLASSIFICATION
UNCLASSIFIED

2a. SECURITY CLASSIFICATION AUTHORITY

3. DISTRIBUTION/AVAILABILITY OF REPORT
UNLIMITED

2b. DECLASSIFICATION/DOWNGRADING SCHEDULE

4. PERFORMING ORGANIZATION REPORT NUMBER(S)
6

5. MONITORING ORGANIZATION REPORT NUMBER(S)

6a. NAME OF PERFORMING ORGANIZATION
ELECTROMAGNETIC APPLICATIONS, INC.

6b. OFFICE SYMBOL (If applicable)

7a. NAME OF MONITORING ORGANIZATION
U.S.ARMY STRATEGIC DEFENSE COMMAND

6c. ADDRESS (City, State, and ZIP Code)
300 COMMERCIAL STREET # 805
BOSTON, MA 02109

7b. ADDRESS (City, State, and ZIP Code)
P.O. BOX 1500, CSSD-AT-E
HUNTSVILLE, AL 35807-3801

8a. NAME OF FUNDING/SPONSORING ORGANIZATION
US ARMY SDI

8b. OFFICE SYMBOL (If applicable)
CSSD

9. PROCUREMENT INSTRUMENT IDENTIFICATION NUMBER
DASG60-92-C-0206

8c. ADDRESS (City, State, and ZIP Code)
P.O.BOX 1500, CSSD-CM-CB
HUNTSVILLE, AL 35807-3801

10. SOURCE OF FUNDING NUMBERS

PROGRAM ELEMENT NO.	PROJECT NO.	TASK NO.	WORK UNIT ACCESSION NO.
	2C2753		

DTIC ELECTE MAR 08 1993 S E D

11. TITLE (Include Security Classification)
DEVELOPMENT OF NOVEL FERRITE ANTENNAS

12. PERSONAL AUTHOR(S)
HOTON HOW

13a. TYPE OF REPORT	13b. TIME COVERED	14. DATE OF REPORT (Year, Month, Day)	15. PAGE COUNT
FINAL	FROM 8/28/92 TO 2/28/93	93/3/1	77

16. SUPPLEMENTARY NOTATION

17. COSATI CODES			18. SUBJECT TERMS (Continue on reverse if necessary and identify by block number)
FIELD	GROUP	SUB-GROUP	PATCH ANTENNAS, FERRITES, THIN FILMS, MICROSTRIP LINES.

19. ABSTRACT (Continue on reverse if necessary and identify by block number)

We have performed and successfully completed a phase I study involving an isolated ferrite patch antenna possessing a circular or a rectangular geometry. The radiation frequencies measured as a function of the biasing magnetic field compared quantitatively with our theory. Measurements on the radiation patterns confirmed the nature of the normal modes of the patch antennas. Ferrite patch antennas may be used for the following purposes: generation of circularly polarized radiations, wide frequency tuning range for single mode application, and RCS reduction on patch antennas.

20. DISTRIBUTION/AVAILABILITY OF ABSTRACT
☒ UNCLASSIFIED/UNLIMITED ☐ SAME AS RPT. ☐ DTIC USERS

21. ABSTRACT SECURITY CLASSIFICATION
UNCLASSIFIED

22a. NAME OF RESPONSIBLE INDIVIDUAL

22b. TELEPHONE (Include Area Code)

22c. OFFICE SYMBOL

DD Form 1473, JUN 86 Previous editions are obsolete. SECURITY CLASSIFICATION OF THIS PA

DISCLAIMER NOTICE

THIS DOCUMENT IS BEST QUALITY AVAILABLE. THE COPY FURNISHED TO DTIC CONTAINED A SIGNIFICANT NUMBER OF COLOR PAGES WHICH DO NOT REPRODUCE LEGIBLY ON BLACK AND WHITE MICROFICHE.

SBIR Phase I Final Report

Accesion For	
NTIS CRA&I	X
DTIC TAB	☐
Unannounced	☐
Justification	
By	
Distribution /	
Availability Codes	
Dist	Avail and / or Special
A-1	

DTIC QUALITY INSPECTED 1

Name of Contractor: ElectroMagnetic Applications, Inc. (EMA)
Contract Number: DASG60-92-C-0206
Effective Date of Contract: August 28, 1992
Expiration Date of Contract: February 28, 1993
Reporting Period: 8/28/92 - 2/28/93
Principal Investigator: Hoton How, (617)720-3968
Project Scientist: Carmine Vittoria, (617)720-3968
Title of Work: Development of Novel Ferrite Patch Antennas

93-04800

93 3 5 021

Table of Contents

I. Introduction

Patch antennas are normally constructed with dielectric substrates. However, by including ferrite materials in the design of patch antennas one may obtain additional control over the radiation of the antenna. Dielectric materials are electrically isotropic, but the response of magnetic materials to magnetic fields may be highly anisotropic. By magnetic materials in this report we mean ferrite materials. Ferrite materials provide tensor permeabilities which can be systematically varied/tuned over a wide frequency range by adjusting the biasing magnetic field. Recently, there has been increasing interest in the study of ferrite patch antennas.[1,2,3,4] In this phase I research we have analyzed exclusively the properties of an isolated or single ferrite patch antenna, both theoretically and experimentally. Specifically, we have fabricated circular and rectangular patch antennas. The antenna were tested from 0.04 to 20 GHz using an HP8510B network analyzer. The radiation frequencies, scattering parameters, and radiation patterns of the antennas were analyzed. The ferrite materials included in the design of the antennas were characterized in static magnetic fields. The above measurements were compared with calculations performed by us. The calculations were based upon a novel formulation developed by us for the first time. Previous calculations were inadequate in analyzing data generated from ferrite patch antennas. In summary the first prototype ferrite patch antenna was fabricated and tested by us and also we developed a novel analysis applicable for ferrite patch antennas. Application of ferrite patch antennas include the following:

1. Magnetic Tuning of the Radiation Frequencies - The most evident application for a ferrite patch antenna is probably due to its field-dependent magnetic permeability. This provides a convenient way of designing a frequency-tunable microstrip patch antenna. We found that frequency tuning can be applied to ferrite patch antennas possessing circular or rectangular geometry. For rectangular ferrite patch antennas the range of frequency tuning can be very wide in which single mode operation is possible. The ability that the radiation frequency can be tuned via the biasing magnetic field may find immediate applications for frequency modulation.

2. Circularly Polarized Radiations - Conventional circularly polarized antennas are designed as either single-fed elliptic patches or dual-fed rectangular patches. For single-fed elliptic patches the amount of ellipticity of the patch geometry controls the mixing of the two orthogonal linearly-polarized radiations, which in turn gives rise to the circularly polarized waves.[5] For dual-fed rectangular patches two orthogonal feeds are required in which the relative phases are shifted 90° apart from each other.[6] Ferrite patch antennas irradiate circularly polarized waves, since the precessional motion of the magnetization is circularly polarized. In the absence of a magnetic field the precessional motion can be either left or right circularly polarized. The degeneracy is removed upon the application of a magnetic field. This means that at one frequency the precessional motion is left circularly polarized, but opposite at another frequency. Thus, it is possible at two different frequencies to radiate energy with

opposite sense of circular polarization. One potential application of this effect is to use the antenna in an IFF (Identification for Friendly and Foe) system in which a ferrite patch antenna can emit an identification signal after receiving a signal at the other frequency whose sense of polarization is opposite to the transmitted signal.

3. Reduction in the Radar Cross Section on the Antenna - Radar Cross Section (RCS) of an object means the effective (not physical) area of the object being detected by a radar. Therefore, the smaller the RCS, the less visible the object to the radar. We observed in this phase I research that the RCS area of a patch antenna can be greatly reduced (by a factor of 10 dB) by incorporating a composite structure of ferrite materials. While the substrate is responsible for radiation, the overlay ferrite is tuned at cutoff such as to effectively absorb the incident electromagnetic energy. As such, the antenna is less likely to be detected, and, hence, results in increased survivability.

The above features are unique to a ferrite patch antenna. The other important application involving ferrite patch antennas is for electronic steering of radiation beams. Traditional electronic steerable patch arrays are constructed using electronic delay lines. However, at millimeter wavelength (MMW) frequencies the dimension is small and the adjustment of the amount of phase shifts for a big array becomes a formidable task. The design of ferrite conformal arrays can be relatively simple, inexpensive, and robust. They may be readily used for nondestructive evaluation of materials and for vehicle collision avoidance in the commercial world. Detailed description of using ferrite patch antenna arrays will be presented in a future phase II proposal.

The work performed in the phase I period has been included in the writeup of two papers: "Radiation Frequencies of a Microstrip Antenna on a Ferrite Substrate,[7]" and "Intrinsic Modes of Radiation in Ferrite Patch Antennas.[8]" They are attached to this final report in the Appendices and are intended to be published in the journals of Electronics Letters and IEEE Transactions on Microwave Theory and Techniques. Clearance is needed from the sponsoring agency.

II. Summary of Work

Two kinds of ferrite substrates have been used in the fabrication of ferrite patch antennas. They are magnesium ferrite (TT1-1000) and yttrium iron garnet (G-1010), both of which were purchased from Trans-Tech, Inc.. The substrates are of dimension $0.02" \times 0.2" \times 0.2"$ and their properties are summarized in Table 1. Table 1 also contains the parameters of fourteen ferrite patch antennas, 8 circular and 6 square, which were fabricated and tested during the phase I period. Fig.1 shows the photograph of these fourteen elements. Patch antennas were fabricated using the photolithography and wet etching techniques.

For the S_{11} measurements we have used an electromagnet which provided biasing magnetic fields for the ferrite substrate up to 9 kOe. The field can be applied either in the plane or normal to the plane of the substrate. As such, the resonant frequencies of the patch antenna for both field biasing configurations can be determined. In order to measure the radiation profile and polarization we have used small permanent magnets in biasing the ferrite substrates. For the parallel field case we used two permanent neodymium magnet discs of diameter 0.5" and height 0.19" which were arranged face-to-face directly below the ferrite substrate (beneath the ground plane). This produced transverse magnetic field for the substrate in the order of 2 kOe. For the normal field case we have designed a special pedestal for the substrate which allowed for continuous change in the biasing field strength. As shown in Fig.2, the magnet disc was enclosed in an aluminum container with screws whose position can be adjusted relative to the ferrite substrate. If a second magnet disc was used on the other side of the patch, a normal biasing field was obtained in the order of 5 kOe. However, if only the bottom magnet was used in biasing the ferrite substrate, the maximum field obtainable was about 3.5 kOe.

Both S_{11} and S_{21} data were taken using a network analyzer HP8510B which was connected to an HP computer. In Sec.III we report measurements on circular ferrite patch antennas where the biasing fields were applied normal to the substrate. A theory was developed by us for the first time to calculate the radiation frequencies of the patch antenna. Sec.IV reports on data obtained on rectangular ferrite patch antennas in which the biasing fields were applied along the edge of one side of the patch. Theory, which is too complex and unyielding to be presented in this report, can be found in Ref.8. In Sec.V we report the data on RCS reduction for ferrite patch antennas with circular geometry. We suggest future work in Sec.VI, which is then followed by a conclusions section , Sec.VII.

III. Circular Ferrite Patch Antennas

1. General Discussion

One may assume the ferrite patch as an insulated resonator where electric walls are bounded from above and below the patch and insulation walls at the periphery of the ferrite patch antenna. An insulation wall is defined as the conditions at which no electromagnetic energy can flow across the wall. This implies that the normal component of the Poynting vector vanishes at an insulation wall. We note that an electric wall or a magnetic wall is an insulation wall, but an insulation wall is not necessarily an electric wall or a magnetic wall. For circular ferrite disc resonator with normal biasing magnetic field the intrinsic normal modes are circularly polarized precessional modes of the magnetization vector. This results naturally into circularly polarized radiations. When the field is removed, the two precessional modes, left and right, become degenerate which combine to emit linearly polarized radiations. Only when the external field is applied to the patch can the two precessional modes irradiate at two distinct and different resonant frequencies.

Fig.3 shows the geometry of a microstrip patch antenna of circular geometry. The radius of the patch is R which is fed by a microstrip line of width w. The external field, H_o, is applied normal to the patch. The coordinates used for describing the patch antenna are also shown in Fig.3. The metal patch is deposited on a ferrite substrate whose thickness, dielectric constant,, FMR line width, and saturation magnetization are denoted as d, ϵ, ΔH, and $4\pi M_s$, respectively. Denote μ and κ as the diagonal and off-diagonal elements of the Polder permeability tensor. One may obtain the following expression for μ and κ:

$$\mu/\mu_o = 1 + f_m f_1[f_1^2 - f^2(1 - \alpha^2)]/\{[f_1^2 - f^2(1 + \alpha^2)]^2 + 4f_1^2 f^2\alpha^2\}, \quad (1)$$

$$\kappa/\mu_o = f_m f[f_1^2 - f^2(1 - \alpha^2)]/\{[f_1^2 - f^2(1 + \alpha^2)]^2 + 4f_1^2 f^2\alpha^2\}, \quad (2)$$

where f is the frequency, $f_1 = \gamma H_{in}$, $\gamma = 2.8$ MHz/Oe if the spectroscopic splitting factor $g_{eff} = 2.0$, H_{in} is the internal magnetic field, $f_m = \gamma 4\pi M_s$, and $\alpha = \gamma\Delta H/2f$. One may approximate the ferrite disc as an oblate spheroid with eccentricity e given by

$$e = (4R^2/d^2 - 1)^{1/2}. \quad (3)$$

The internal field H_{in} can then be estimated as

$$H_{in} = H_o - 4\pi M_s N_z \quad (4)$$

with the axial demagnetizing factor N_z given by

$$N_z = (1 + e^2)(e - \tan^{-1}e)/e^3. \quad (5)$$

The effecitve permeability, the Voigt permeability, is

$$\mu_v = (\mu^2 - \kappa^2)/\mu \quad (6)$$

and the wave propagation constant is

$$k = 2\pi f(\epsilon\mu_v\epsilon_o\mu_o)^{1/2}. \quad (7)$$

The radiation frequencies of the ferrite antenna can be determined from the following equation

$$J_n'(x) - (\kappa/\mu)nJ_n(x)/x = 0, \quad (8)$$

where $x = kR$, and $J_n(x)$ and $J_n'(x)$ are Bessel function of the first kind with order n and the

derivative of $J_n(x)$ with respect to x, respectively. Note that n can be positive integers, left precessional motion, or negative integers, right precessional motion. The above formulas apply only if H_{in} is greater than zero, i.e., the substrate is magnetically saturated. For an unsaturated substrate we have $H_{in} = 0$, and the saturation magnetization $4\pi M_s$ shall be replaced by H_o/N_z.

2.Radiation Pattern

Figs.4 to 7 show S_{11} and S_{21} measurements for a circular ferrite patch antenna deposited on a magnesium ferrite substrate, 2R = 1.27 cm, ferrite patch antenna #2. Other circular patches show similar behaviors. Figs.4 and 5 were measured in the absence of a biasing magnetic field, and Figs.6 and 7 were biased by a normal magnetic field of 788 Oe. For the S_{21} measurements the receiver waveguide horn antenna was located directly above the sample antenna to be tested, the z-axis, and the polarization of the horn antenna can be either parallel, Figs.4 and 6, or perpendicular, Figs.5 and 7, to the microstrip feedline, the x-axis. Comparing Figs.4 to 5, it is clear that the circular patch emited linearly polarized radiations in the absence of a biasing field, and the linear dipole direction was parallel to the feedline, the x-axis. However, when a normal field was applied, Figs.6 and 7, the degeneracy between the two circular precessional modes was removed, and the two circular modes resonated at two distinct frequencies. That is, when the degenerate modes resonated at f = 4.97 GHz with zero biasing field, the two modes resonated at different frequencies, f^+ = 5.65 GHz and f^- = 4.39 GHz, when the normal field was increased to 788 Oe. The circular feature of the precessional modes is evident from Figs.6 and 7 where the S_{21} intensities do not depend on the orientation of the detector horn antenna. The radiation fields were circularly polarized. This proves the most important assertion concerning the features of the radiation generated from a circular ferrite patch antenna biased by a normal magnetic field.

The radiation pattern of the circular ferrite patch antenna #2 was measured using the same detector horn antenna which was mounted in an arch (diameter = 2 m) with the sample antenna located at the center of the arch. The arch was rotated around the z-axis which allowed us to profile the radiation pattern in the two principal planes, the x-z plane ($\phi = 0$ plane) and the y-z plane ($\phi = \pi/2$) plane. The detector horn antenna was located in two orientations: copolarized if the detector polarization was in the detector plane, or crosspolarized if the detector polarization was normal to the detector plane. Figs.8 to 15 depict the radiation patterns in the $\phi = 0$ and $\pi/2$ planes associated with the two precessional modes shown in Figs.6 and 7. They were plotted in polar coordinates with the amplitude normalized with respect to that occurring at $\theta = 0°$. From Figs.8 to 15 one may visualize the two precessional modes as being composed of two linearly polarized dipoles of equal magnitude lying in the x and y directions. In order words the two precessional modes are indeed circularly polarized.

3. Radiation Frequency

The radiation frequencies of a circular ferrite patch antenna as a function of the normally biased magnetic field have been studied quantitatively. Fig.16 shows such a plot which was measured on ferrite patch antenna #11 (YIG substrate, 2R = 0.89 cm). From Fig.16 one may distinguish the radiation frequencies in three regions. In region (I) the applied magnetic field was so weak that the ferrite substrate was actually unsaturated. In region (II) the field was below FMR and in region (III) above FMR. The (+) and (-) modes denote left and right hand precessional modes which become degenerate when the biasing field, H_o, vanishes or when H_o achieves infinity. That is, only when $H_o = 0$ or $H_o = \infty$ can the effective permeability of the ferrite, μ_v, equals unity, please see Eqs.(1), (2), and (6). In Fig.16 full dots represent biasing-below-FMR data (including the unsaturated region), and open dots above FMR. The solid lines are theoretical curves calculated from Eqs.(1) to (8) using the following parameters: $4\pi M_s$ = 1023 G, ϵ' = 14.34, ΔH = 48 Oe, and R = 0.41 cm. The $4\pi M_s$, ϵ, and ΔH values are furnished by the manufacturer, please see Table 1, and the patch diameter R is determined by a best-fit algorithm, since the physical dimension of the patch does not imply the physical dimension of the embedded cavity resonator.

In Fig.16 only the fundamental dipole modes, $n = \pm 1$, and the fundamental quadrupole modes , $n = \pm 2$, were detected and calculated. Other higher order radial modes for $n = \pm 1$ and $n = \pm 2$ were omitted, since they exhibited very low intensities in the measured S_{11} data compared to the fundamental modes (about 15 dB lower). In Fig.16 one notices the general agreement between theory and experiments. Therefore, we conclude that the radiation frequencies of a circular ferrite patch antenna can be continuously tuned by changing the biasing magnetic field. Single mode operation with a wide frequency tuning range can be best realized in Fig.16 as the $n = +1$ mode biased below FMR, although we believe that $n = +1$ mode biased above FMR, which is only partly shown in Fig.16, is equally good for single mode operations.

IV. Rectangular Ferrite Patch Antennas

1. General Discussion

In the past we have reported on a theory which calculated the normal mode frequencies of a microstrip patch antenna on a "magnetically unsaturated" ferrite substrate.[1] During the phase I work we have extended the theory to patch antennas consisting of ferrite substrates which are magnetically saturated.[7,8] Fig.17 shows the geometry of a microstrip patch antenna of square geometry. The length of the square is a and a microstrip line of width w is fed into the antenna at the center of one side of the patch. The biasing magnetic field, H_o, is applied along one side of the patch and perpendicular to the microstrip feed line. The coordinates used for describing the patch antennas are shown in Fig.17 which are different from that used for describing circular patch antennas, please see Fig.3. Procedures for solving the intrinsic modes of radiation frequencies in a rectangular ferrite patch antenna are as follows: we first construct the

propagation modes in a parallel plate waveguide loaded with a ferrite slab of the same thickness, d. The top square patch of the antenna is temporarily replaced by an infinite conducting sheet. The normal mode solutions of the finite ferrite cavity can then be composed as superpositions of the propagation modes of the waveguide, provided that boundary conditions are satisfied at the periphery of the cavity. For dielectric patches one normally assumes magnetic wall boundary conditions at the patch periphery.[6] However, for a ferrite patch antenna magnetic wall boundary conditions can not give rise to proper solution of the radiation frequencies, since this boundary condition gives rise to trivial solutions in which the electromagnetic fields vanish everywhere in the cavity. We suggested the use of the so-called "insulation wall" boundary condition. We define an insulation wall to be the conditions at which no electromagnetic energy can flow across the wall. This implies that the normal component of the Poynting vector vanishes at an insulation wall. We note that an electric wall or a magnetic wall is an insulation wall, but an insulation wall is not necessarily an electric or a magnetic wall.

A full derivation of the normal mode solutions within a ferrite cavity can be found in Ref.8. Here we summarize the properties of the normal mode solutions of the radiation frequencies which are compared with experimental data. One may distinguish three types of normal modes. The first type is the dielectric or the uncoupled mode. For the uncoupled mode the rf h-field is parallel to the dc applied field which are both perpendicular to the wave propagation direction of that mode. As such, there is no magnetic coupling and the effective permeability value is 1. For the second type of normal mode, or the so-called Voigt mode, the rf h-field, the dc magnetic field, and the propagation direction are all perpendicular to each other. The Voigt modes are therefore referred to as the transverse TE modes. The Voigt permeability is given by[8]

$$\mu_v = 1 + 4\pi M_s(4\pi M_s + H_o)/(H_o^2 + 4\pi M_s H_o - f^2/\gamma^2). \qquad (9)$$

Voigt modes are continuous modes, since the normal mode frequencies can be continuously tuned by varying the external biasing magnetic field, H_o.

The third type of normal modes are longitudinal TE modes whose propagation direction is along the dc field. Longitudinal TE modes form discrete modes (subject to no frequency-tuning capability) and require nodal points in the z-direction. This is in contrast to the former two types of normal modes which assume no field variation along the z-direction. Formation of longitudinal TE mode is similar to the internal reflection of electromagnetic waves in a birefringent medium; the ordinary and the extraordinary waves form standing waves in the z-direction involving different number of nodal points. The longitudinal TE modes appear near the region of ferrimagnetic resonance (FMR). We note that all of the three types of normal modes result in linearly polarized radiations in the far zone. The polarization axis of a Voigt mode is orthogonal to that associated with the other two types of normal mode radiations.

2. Radiation Pattern

Figs.18 an 19 shows the measured radiation pattern of ferrite patch antenna #6 (magnesium ferrite substrate, a = 0.95 cm) in the two principal planes $\phi = 0$ and $\phi = \pi/2$. We have used two neodymium discs in biasing the ferrite substrate. The two magnets were brought face-to-face under the ground plane which produced a transverse magnetic field in the order of 2 kOe. In Figs.18 and 19 the biasing field was 2010 Oe, and the radiation frequency was 9.51 GHz. Similar radiation patterns were also measured for other square ferrite patch antennas. From these measurements we found that for square ferrite patch antennas main radiations are copolarized in the $\phi = 0$ plane and crosspolarized in the $\phi = \pi/2$ plane. Other polarizations were about 10 dB below the main radiations. This verifies the transverse nature of the Voigt modes. From Figs.18 and 19 we conclude that the main radiations, the Voigt modes, constitute linear dipoles whose polarization are perpendicular to the microstrip feed line. For ferrite patch antenna #6 we have also measured similar radiation patterns for the dielectric mode at f = 4.93 GHz and the longitudinal TE mode at f = 5.91 GHz and H_o = 1470 Oe. However, the polarization patterns were rotated 90° away from those of Figs.18 and 19, and the measured intensities were about 10 dB lower than the main radiations of the Voigt modes.

3. Radiation Frequency

In Fig.20 the radiation frequencies of the ferrite patch antenna #6 are shown as a function of the biasing magnetic field. The ferrite antenna was inserted in an electromagnet which provided magnetic fields up to 9 kOe. The field was along the edge of ones side of the square patch perpendicular to the microstrip feed line.S_{11} data were taken using a network analyzer (HP8510B) which was connected to an HP computer. In Fig.20 full dots represent biasing below-FMR data, and open dots above FMR. The dashed lines are purely dielectric or uncoupled modes whose frequencies are independent of the applied field. The intensities as measured in changes in S_{11} of the dielectric or uncoupled modes were observed mostly for magnetic fields below FMR. The solid lines in Fig.20 are theoretical curves for the Voigt modes calculated from Eq.(9) using the following parameters: $4\pi M_s$ = 985 G, ϵ = 11.41, and a = 0.91 cm. The $4\pi M_s$ and ϵ values are furnished by the manufacturer, please see Table 1, and the patch dimension, a, was determined by a best-fit algorithm, since the patch dimension of the patch (0.95 cm) does not imply the dimension of the embedded cavity resonator. A discrete data point, solid diamond, is also shown in the near-FMR region of Fig.2 reminiscent of the longitudinal TE mode. Since the longitudinal TE mode exhibited very low intensity, other high order longitudinal TE modes were not observed in the present S_{11} measurements. In Fig.20 the agreement between theory and experiments is good.

We conclude that Voigt modes in rectangular ferrite patch antennas might have potential for important engineering applications. For example, Fig.20 shows the possibility for wideband frequency tuning capability involving single mode operation. That is, the fundamental mode for biasing-below-FMR can be roughly single-mode-tuned from 5 to 10 GHz, octave bandwidth in

frequency tuning, by varying the field from 0 to 2.5 kOe.

V. Radar Cross Section Reduction for Ferrite Patch Antennas

We have developed a unique configuration for ferrite patch antennas which achieves the following advantages in one design: radiation frequency tunability, circularly polarized electromagnetic radiations, and reduction in antenna radar cross section (RCS). We have utilized two ferrite materials in the antenna design, one ferrite substrate and one ferrite disc, which possess different saturation magnetizations. Hence, the ferrimagnetic resonance (FMR) frequencies are different for the two ferrite materials. The radiation frequency of the antenna originated from the patch resonance within the ferrite substrate which was biased away from the FMR of its own, denoted as FMR_s. The second ferrite disk was placed on top of the patch whose FMR, denoted as FMR_t, located at the radiation frequency of the ferrite patch antenna. As such, the antenna's RCS is reduced, since an incident electromagnetic wave sent by a second radar will be significantly absorbed by the top ferrite operating at cutoff. All of the above operations are subject to frequency tunability, since the two ferrites are simultaneously biased by a common magnetic field.

Figs.21 and 22 shows the S_{11} and S_{21} data for the circular ferrite patch antenna #2 (magnesium ferrite, 2R = 1.27 cm) biased above FMR. In Fig.21 there was no ferrite disc placed above the circular patch and there is only one FMR absorption peak observed in the S_{11} data, denoted as FMR_s in Fig.21. The biasing magnet was a permanent neodymium disc located under the substrate which provided a normal magnetic field of 3410 Oe. The S_{21} measurements were performed using a detector waveguide horn antenna which was mounted right above the sample antenna with an orientation parallel to the microstrip feed line. It is seen that the two precessional modes resonate at two distinct frequencies f^+ = 4.52 GHz and f^- = 3.67 GHz as discussed previously in Sec.III. Fig.22 shows the same measuring configuration as Fig.21 except that a second permanent magnet was place on top of the circular patch of the ferrite microstrip antenna. The top magnet serves as another ferrite substance which produced a second line of FMR absorption in the S_{11} data, denoted as FMR_t in Fig.22. Two effects are noticed as a consequence of the top ferrite. Firstly, the two radiation modes resonating at f^+ and f^- were mixed to form a single broad band radiation. Secondly, the S_{11} values of the radiation modes were lowered by an amount of about 10 dB. Since the RCS of the patch antenna can be viewed as roughly proportional to this measured S_{11} data, we conclude that the RCS of the patch antenna has been reduced by a factor of 10 dB due to the FMR absorption of the top ferrite disc. Fig.23 shows the same measurements of Fig.22 plotted in a different frequency window, and Fig.24 shows the measurements where the detector polarization was oriented perpendicular to the microstrip feed line. Comparing Figs.24 to 23, one recognizes that the radiation modes were circularly polarizaed as expected from Sec.III.

VI. Suggestion for Future Work

Present day research into electronically controlled phased arrays has shown that high costs, susceptibility to damage, repairability and so on are problematical issues that will remain in the immediate future. As such there is considerable interest in developing simpler, more robust technologies for particular applications. The use of ferrite materials in antenna apertures as either a radiator or scatterer is one relatively undeveloped technique for providing electronic control, although its deployment in discrete phase shifting components is well known. More recently, with the availability of improved ferrites and compact permanet magnetic circuits, several ferrite -loaded antenna configurations have been reported with varying degrees of beam scanning capabilities.[9,10] In this final report we suggest two ways of achieving two-dimensional steerable beams at millimeter wavelength with potential for conformal applications.

Fig.25 shows a dielectric image-line feeding a slot-antenna array. The slot, which can be either rectangular or circular, are cut on the ground plane which is deposited on the ferrite substrate. The slots are coupled to the dielectric image lines, and the radiated electromagnetic field is directly related to the magnetization state of the ferrite substrate. From previous studies in Japan[9] it has been shown that the radiation beam from such an array can be steered by varying the external magnetic field. In Ref.9 ferrite image lines were used as leaky-wave radiators where the ferrite was biased by a magnetic field along the propagation direction. By changing the strength of the field the radiation beam can be scanned in the radial direction and the scanning rate was reported to be 1°/340 Oe at 50 GHz. We expect the same working principle for a two dimensional array as shown in Fig.25. That is, by changing the magnitude of $H_{DC\perp}$ the beam can be steered in the transverse direction, whereas the change of $H_{DC//}$ results in steering in the longitudinal direction. Basically, the magnitude and direction of H_{DC} may be variable in this application.

Fig.26 shows a two dimensional array of ferrite scatterers deployed in front of an MMW waveguide horn antenna. The ferrites are in the form of thin discs which are glued on a sheet of Teflon or plastic for the purpose of suspension. The external magnetic field is provided for steering the radiation beam from these scatterers. In the past one dimensional ferrite-scatterers array have been fabricated and tested.[10] It was shown that the scattered radiation can be steered by an external field and the scattering angles take discrete values. The steering rate was quite high ($\sim$ 1°/Oe). We expect that the two dimensional ferrite scatterers shown in Fig.26 will work in a similar way. One may want to increase the number of scatterers in the two dimensional array of Fig.26 such as to minimize the scattering angle, and, hence, increase the scanning resolution.

The most important advantage of using ferrite elements in the conformal array design is that it eliminates totally the need for electronic delay lines. At MMW frequencies the wavelengths are small and the adjustment of the amount of phase shifts for a big array becomes a formidable

task. The design of ferrite conformal arrays outlined in Figs.25 and 26 are relatively simple, inexpensive, and robust. Another application for this two dimensional array of ferrite discs is the following. They may be readily used for nondestructive evaluation of materials and for vehicle collision avoidance. Further advantages of using ferrite patch antenna arrays will be reported in a future Phase II proposal.

VII. Conclusions

We have performed and successfully completed a phase I study involving an isolated ferrite patch antenna possessing a circular or a rectangular geometry. The radiation frequencies measured as a function of the biasing magnetic field compared quantitatively with our theory. Measurements on the radiation patterns confirmed the nature of the normal modes of the patch antennas. Ferrite patch antennas may be used for the following purposes: generation of circularly polarized radiations, wide frequency tuning range for single mode application, and RCS reduction on patch antennas. None of the above features can be obtained from a traditional dielectric patch antenna. We have therefore established a basis for future use of ferrite patch antennas, which will no doubt aid the future design of ferrite patch antennas. We believe that we have accomplished the goal that we initially proposed for this phase I work. Future work on ferrite patch antennas should be focused on phased array work. We believe that this will form the most important applications for ferrite patch antennas in the future. Since the phase on each ferrite element in an array can be tuned by an external magnetic field, the radiation beam from the array can be therefore steered. We will propose to continue a phase II study in this direction, which will result in commercial/military applications.

VIII. References

1. H. How, P. Rainville, F. Harackiewicz, and C. Vittoria, "Radiation Frequencies of Ferrite Patch Antennas," Electronics Letters Vol.28, 1405 (1992).
2. D. M. Pozar and V. Sanchez, "Magnetic Tuning of Microstrip Antenna on a Ferrite Substrate," Electronics Letters, Vol.24, 729 (1988).
3. J. S. Roy, P. Vauson, A. Reineix, F. Jecko, and B. Jecko, "Circularly Polarized Far Fields of an Axially Magnetized Microstrip Antenna", MIcrowave and Optical Technology Letters, Vol.5, 228 (1992).
4. D. M. Pozar, "RCS Reduction for a Microstrip Antenna Using a Normally Biased Ferrite Substrate," IEEE Microwave and Guided Wave Letters, Vol.2, 196 (1992).
5. L. C. Shen, "The Elliptical Microstrip Antenna with Circular Polarization," IEEE Trans. Antenna Propagat. Vol.AP-29, 90 (1981).
6. A. G. Derneryd, "A Theoretical Investigation of the Rectangular Microstrip Antenna Element," IEEE Trans. Antenna Propagat. Vol.AP-26, 532 (1978).

7. H. How, D. Guan, and C. Vittoria, "Radiaiton Frequencies of a Microstrip Antenna on a Ferrite Substrate," to be published.
8. H. How and C. Vittoria, "Intrinsic Modes of Radiation in Ferrite Patch Antennas," to be published.
9. H. Maheri, M. Tsutsumi, and N. Kumagai, "Experimental Studies of Magnetically Scaanable Leaky-Wave Antennas Having a Corrugated Ferrite/Slab/Dielectric Layer Structure", IEEE Trans. Antennas Propagat. AP-36, 911 (1988).
10. N. Okamoto amd S. Ikeda, "An Experimental Study of Electronic Scanning by an Antenna Loaded with a Circular Array of Ferrite Rods", IEEE Trans. Antenna Propag. AP-27, 426 (1979).

IX. Table

	Magnesium Ferrite (TT1-1000)**		Yttrium Iron Garnet (YIG) (G-1010)**	
$4\pi M_s$	985 G		1023 G	
ϵ	11.41		14.34	
tanδ	0.0002		0.0001	
ΔH			48 Oe	
g_{eff}	1.99		1.99	
Thickness (d)	0.02"		0.02"	
Circular Ferrite Patch Antenna Diameter (2R)	#1	1.52 cm	#9	1.52 cm
	#2	1.27 cm	#10*	1.27 cm
	#3	0.89 cm	#11	0.89 cm
	#4	0.51 cm	#12	0.51 cm
Square Ferrite Patch Antenna Side Length (a)	#5	0.99 cm	#13	0.99 cm
	#6*	0.95 cm	#14	0.53 cm
	#7	0.53 cm		
	#8	0.38 cm		
Microstrip Feedline Width (w)	0.426 mm		0.333 mm	

*Shown as individual patches at the right portion of Fig.1.
**Trans-Tech, Inc., P.O. Box 69, 5520 Adamstown Road, Adamstown, MD 21710.

Table 1 Parameters of the fabricated ferrite patch antennas.

X. Figures

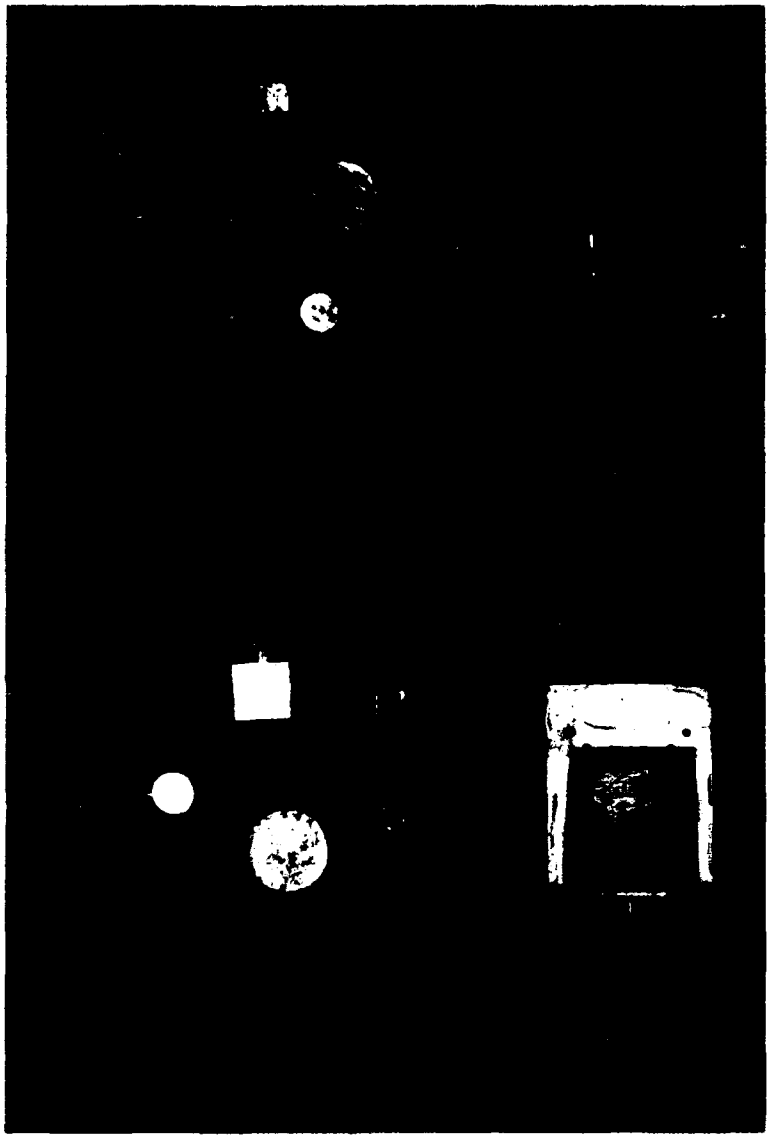

Fig. 1 Ferrite patch antennas fabricated and tested during the phase I period.

Fig.2 Substrate pedestal providing normal bising fields in an adjustable manner.

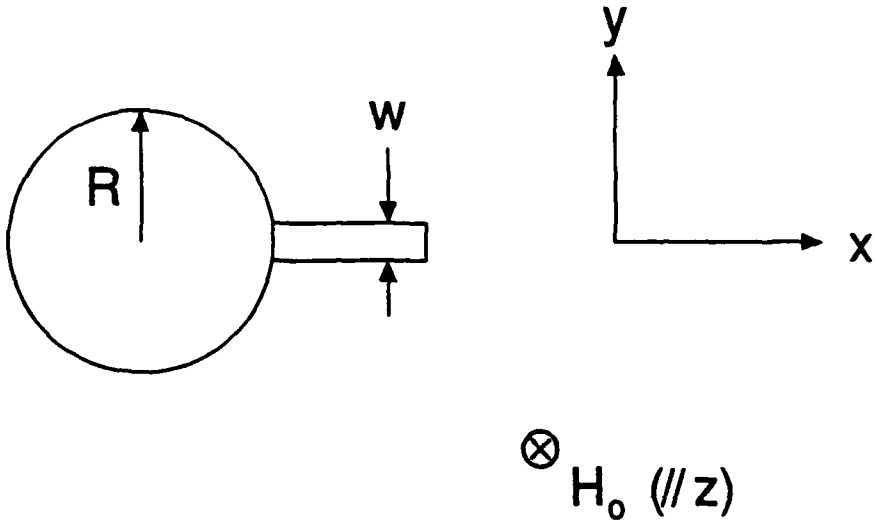

Fig.3 Schematic drawing of the microstrip antenna of circular geometry.

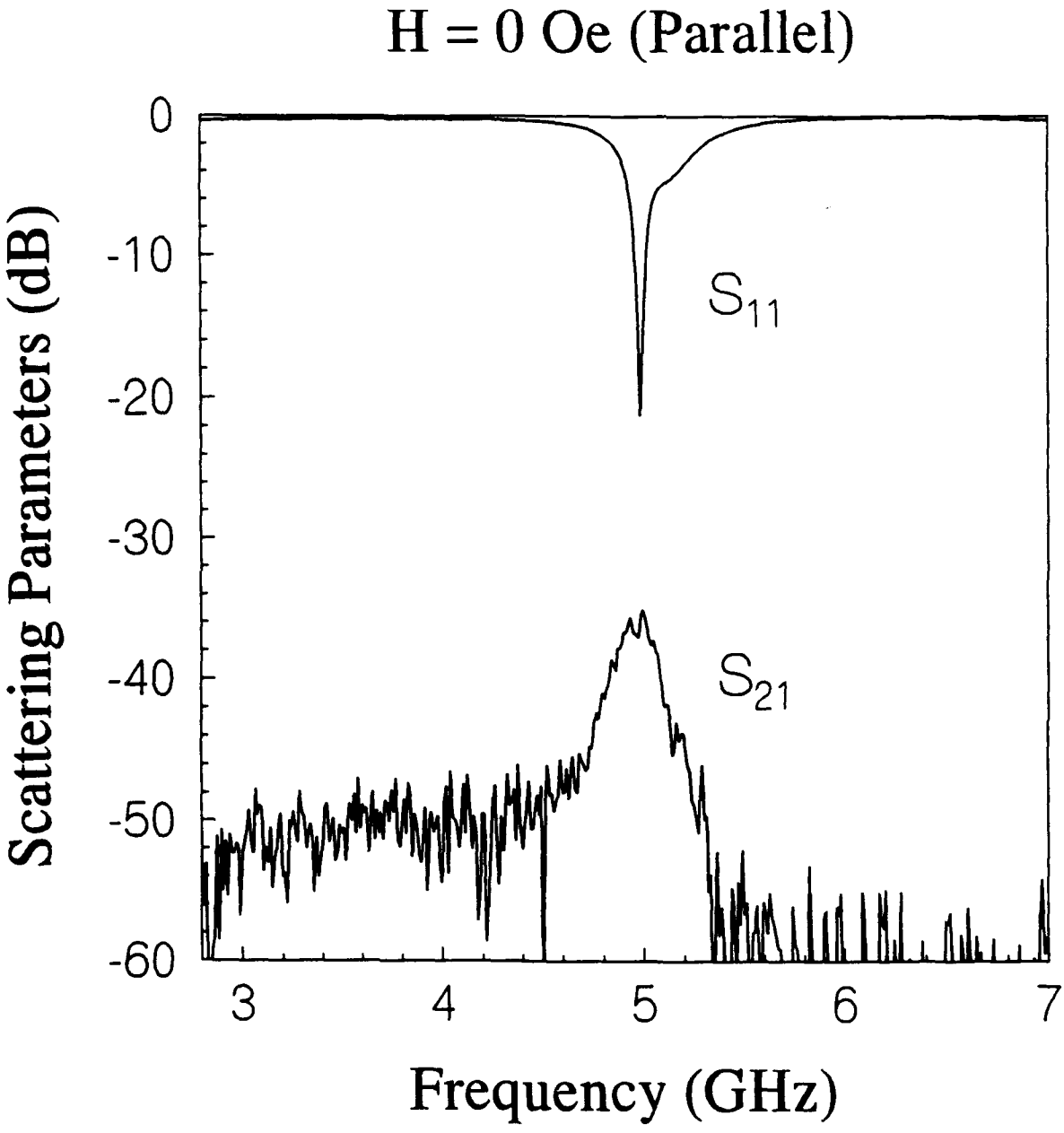

Fig. 4 Measured scattering parameters for ferrite patch antenna #2. The biasing field was 0 Oe and the detector horn antenna was oriented parallel to the microstrip feed line.

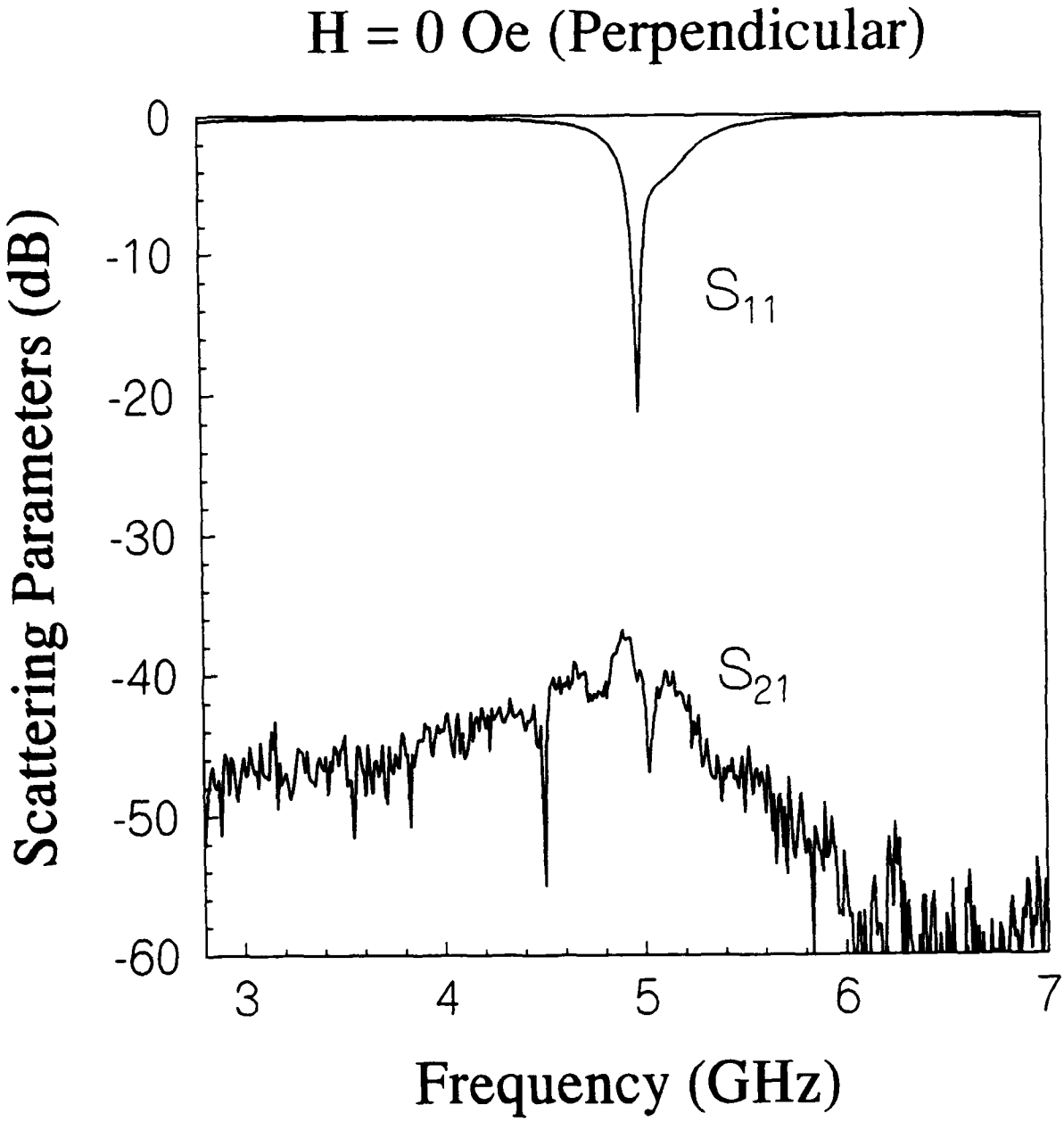

Fig. 5 Measured scattering parameters for ferrite patch antenna #2. The biasing field was 0 Oe and the detector horn antenna was oriented perpendicular to the microstrip feed line.

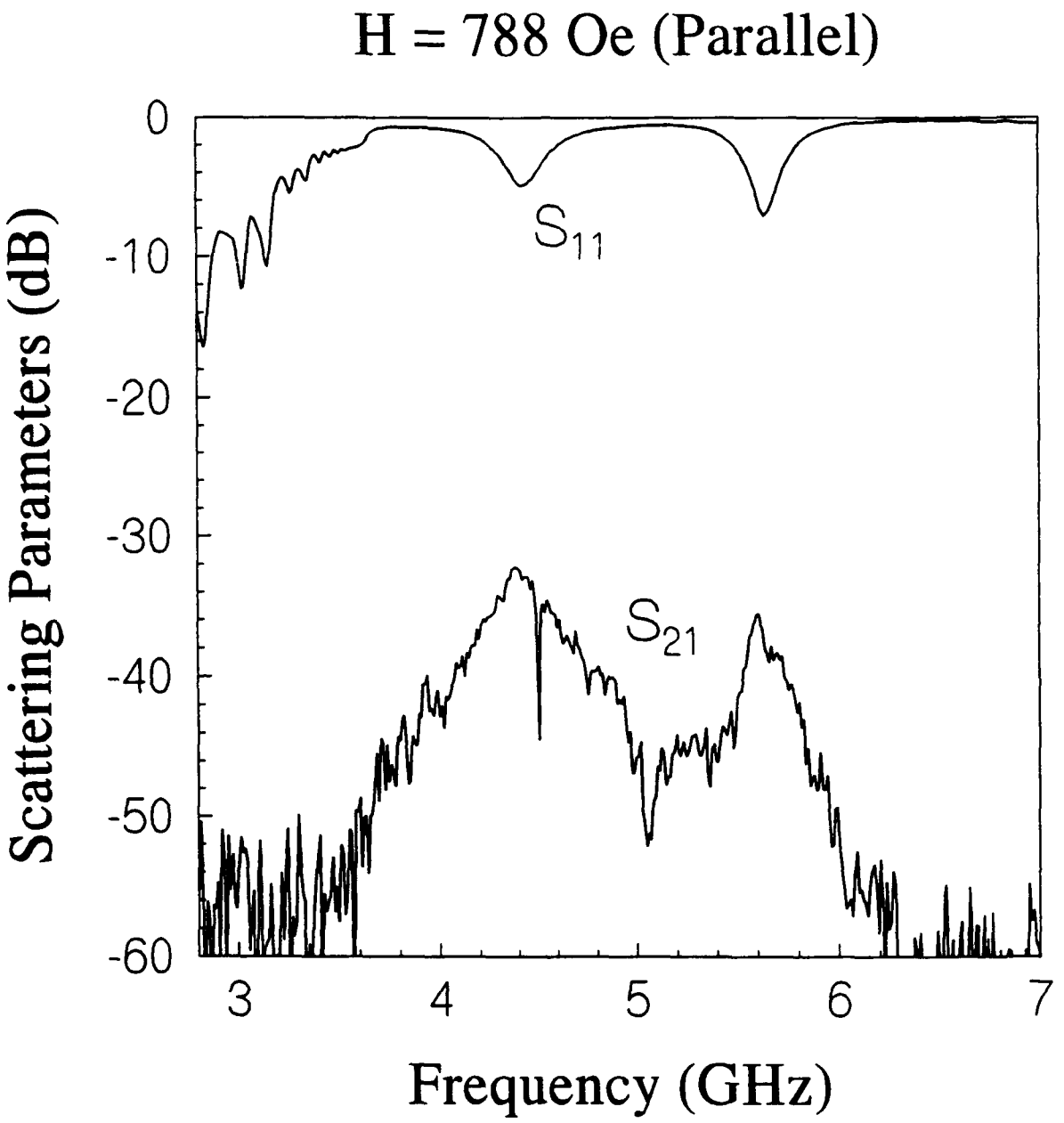

Fig. 6 Measured scattering parameters for ferrite patch antenna #2. The normal biasing field was 788 Oe and the detector horn antenna was oriented parallel to the microstrip feed line.

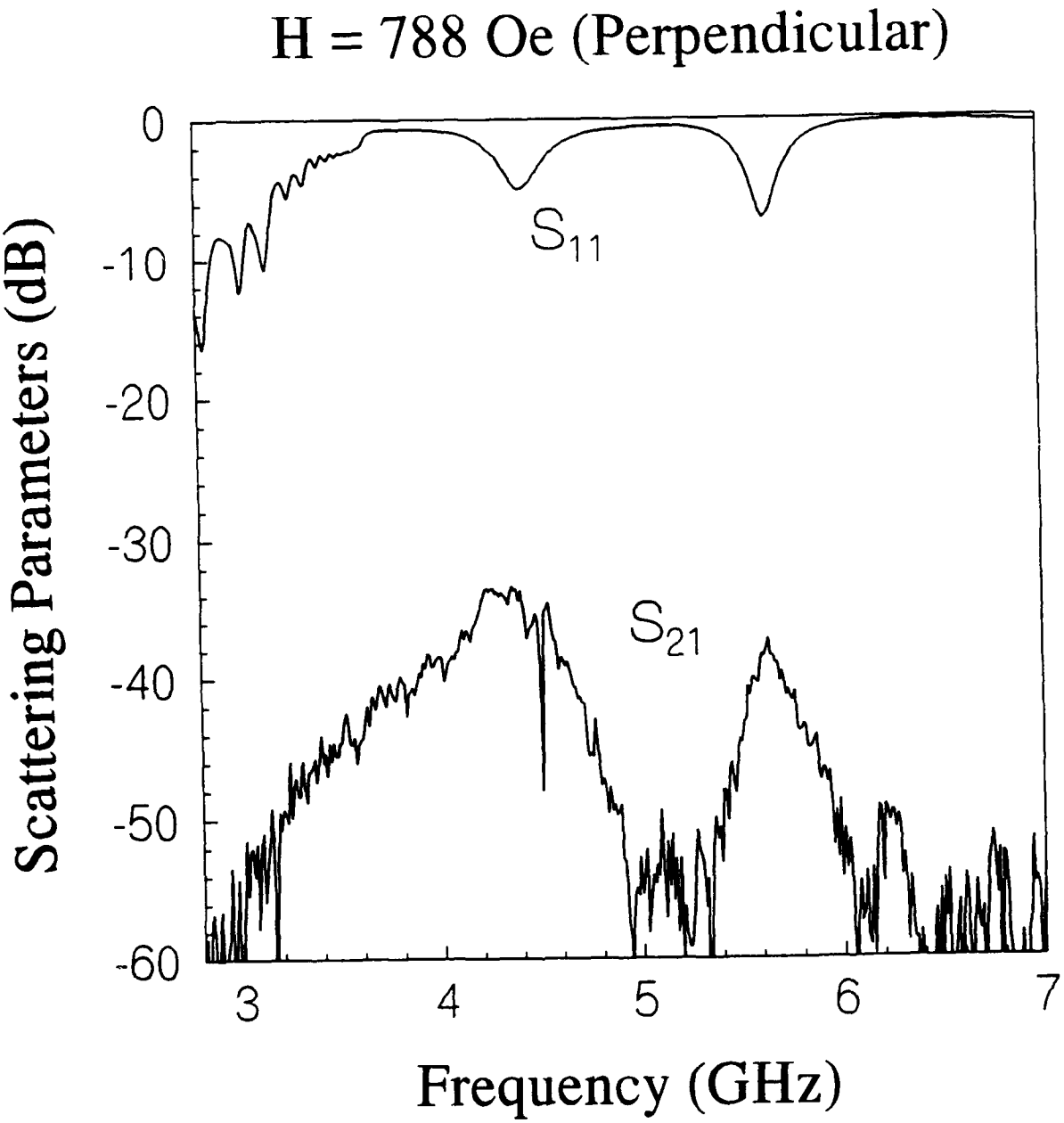

Fig. 7 Measured scattering parameters for ferrite patch antenna #2. The normal biasing field was 788 Oe and the detector horn antenna was oriented perpendicular to the microstrip feed line.

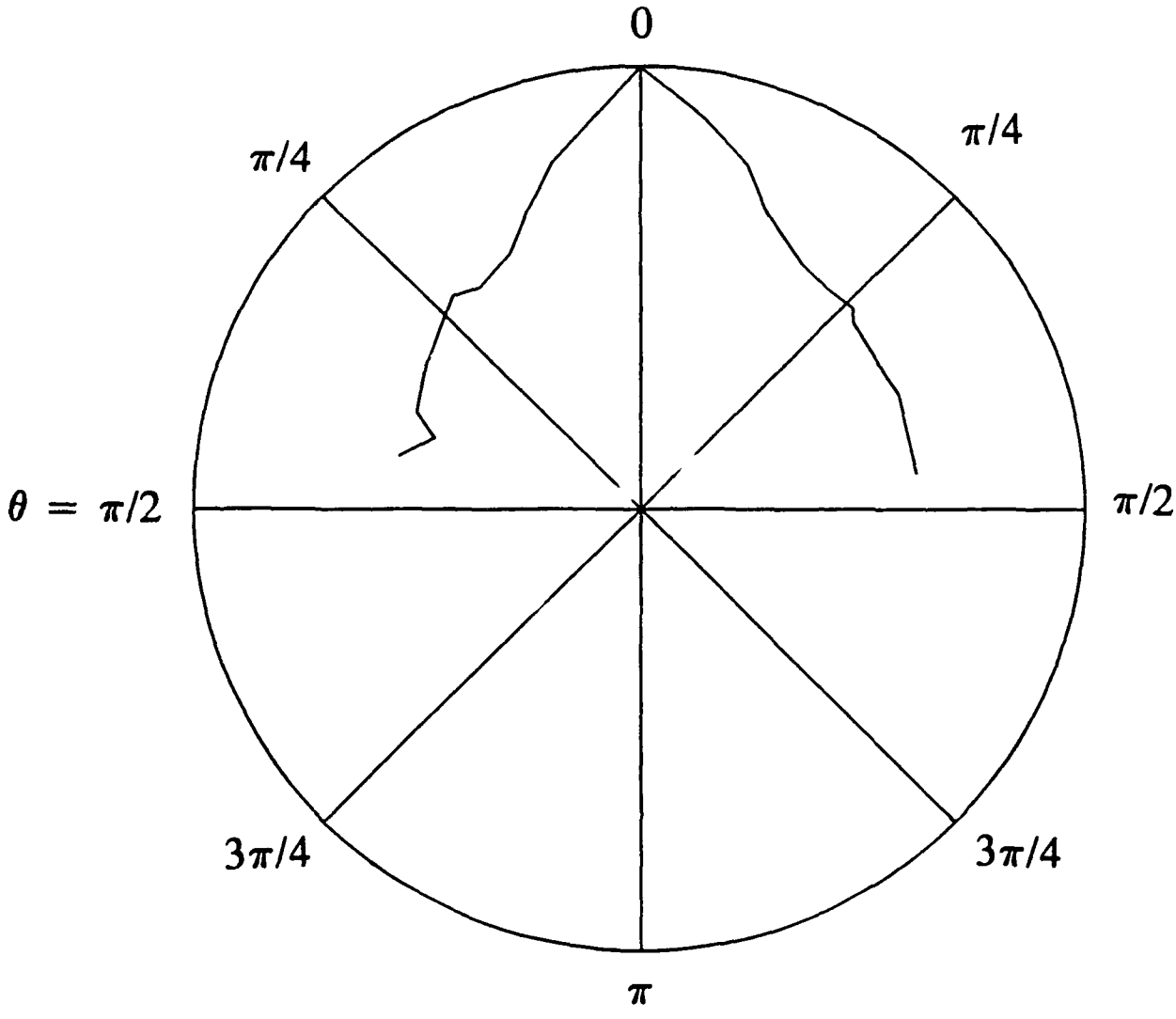

$\phi = 0$ plane: copolarized
(+) mode: f = 5.65 GHz
H_o = 788 Oe

Fig. 8 Radiation pattern for the (+) mode in the $\phi = 0$ plane with copolarized detector orientation.

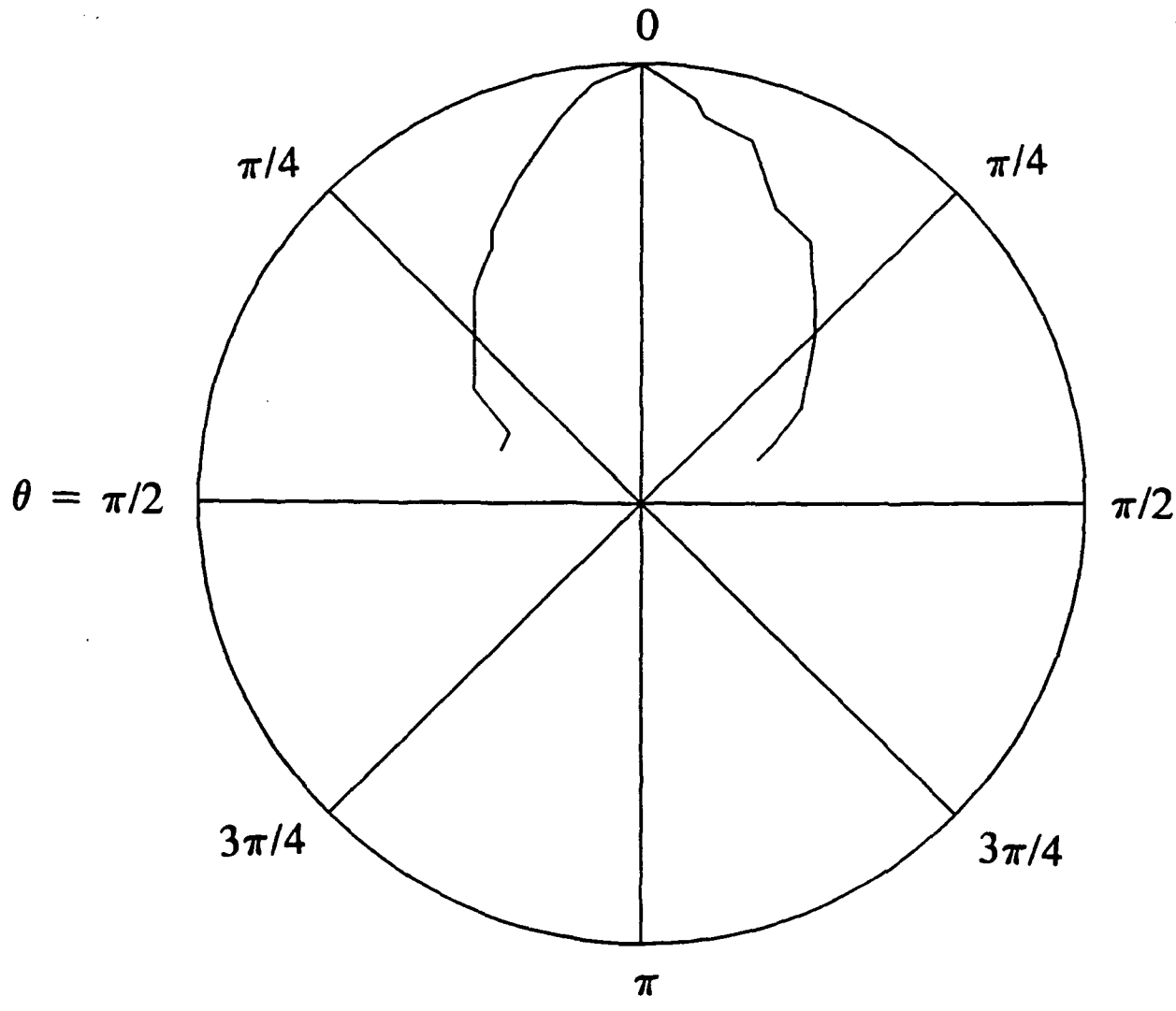

$\phi = 0$ plane: crosspolarized
(+) mode: f = 5.65 GHz
H_o = 788 Oe

Fig. 9 Radiation pattern for the (+) mode in the $\phi = 0$ plane with crosspolarized detector orientation.

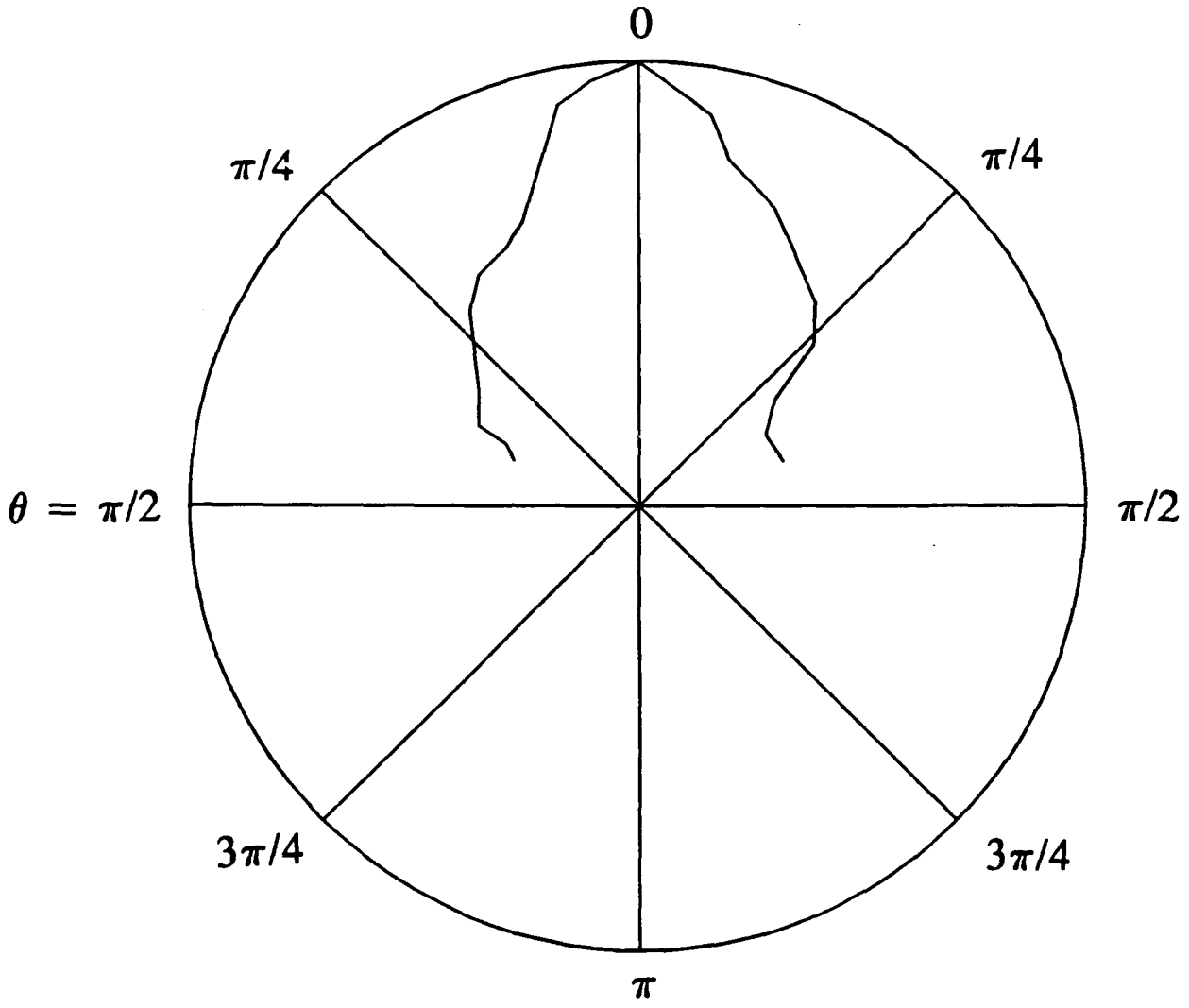

$\phi = \pi/2$ plane: copolarized
(+) mode: f = 5.65 GHz
H_o = 788 Oe

Fig. 10 Radiation pattern for the (+) mode in the $\phi = \pi/2$ plane with copolarized detector orientation.

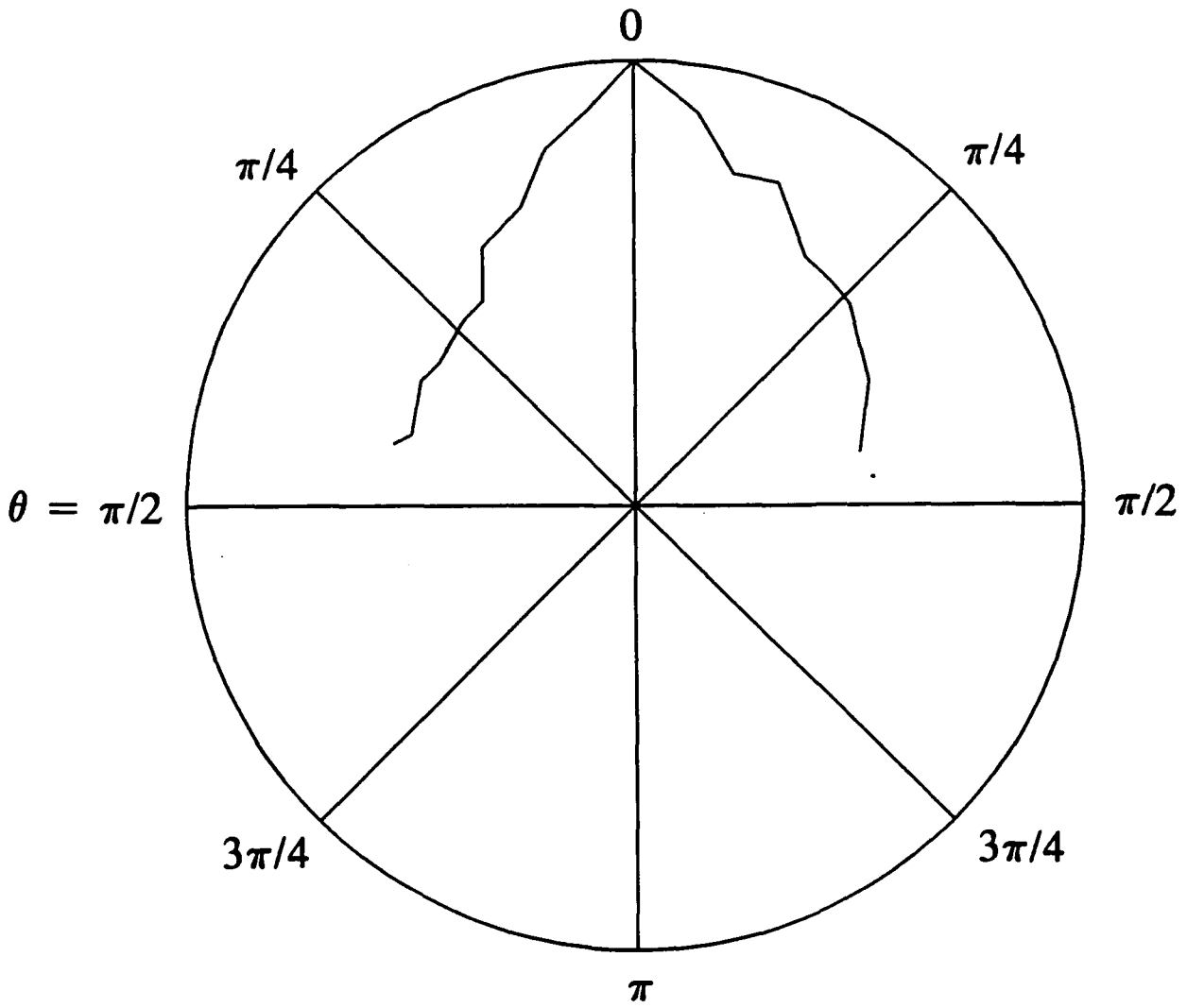

$\phi = \pi/2$ plane: crosspolarized
(+) mode: f = 5.65 GHz
H_o = 788 Oe

Fig.11 Radiation pattern for the (+) mode in the $\phi = 0$ plane with crosspolarized detector orientation.

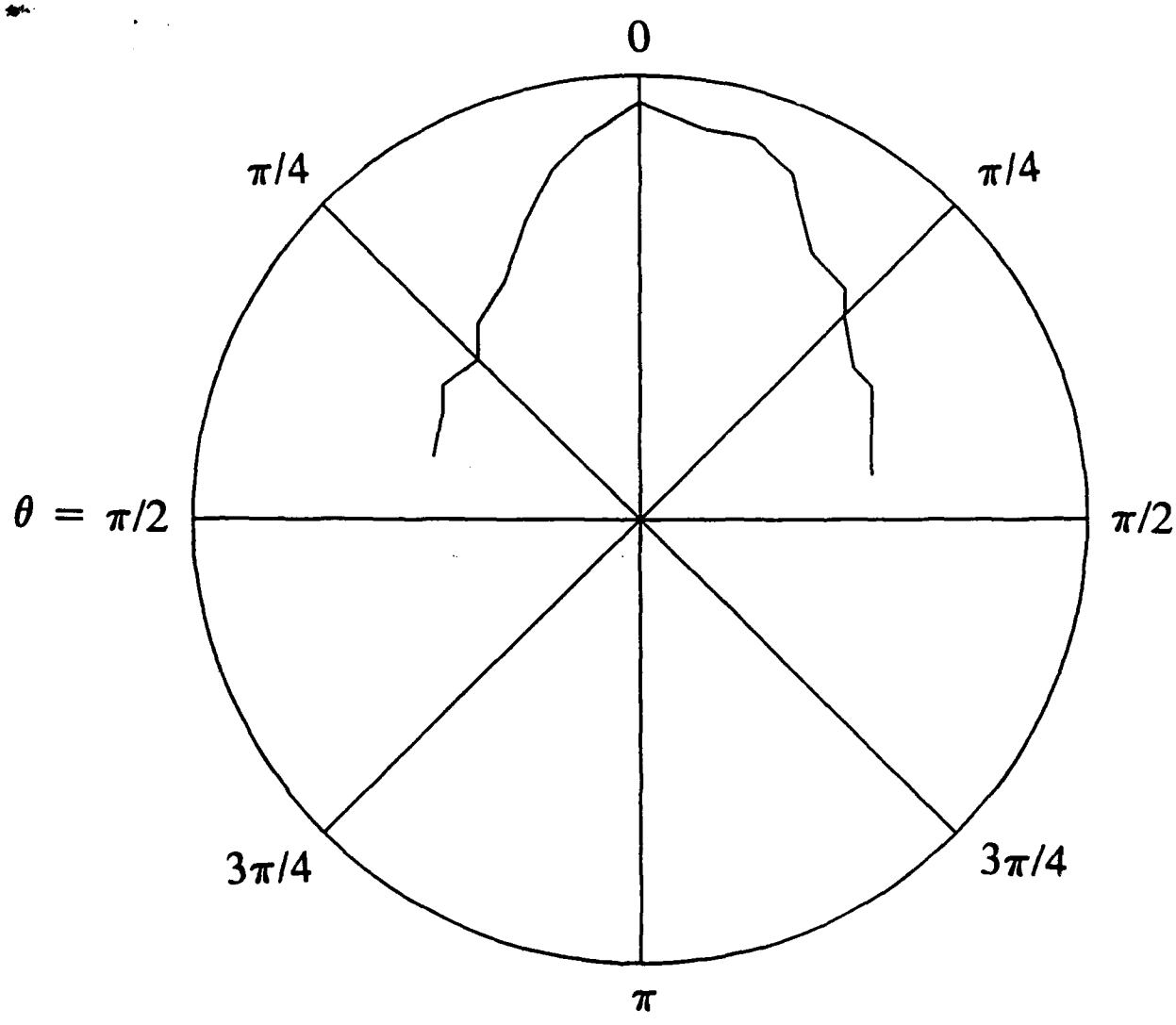

$\phi = 0$ plane: copolarized
(-) mode: f = 4.39 GHz
H_o = 788 Oe

Fig. 12 Radiation pattern for the (-) mode in the $\phi = 0$ plane with copolarized detector orientation.

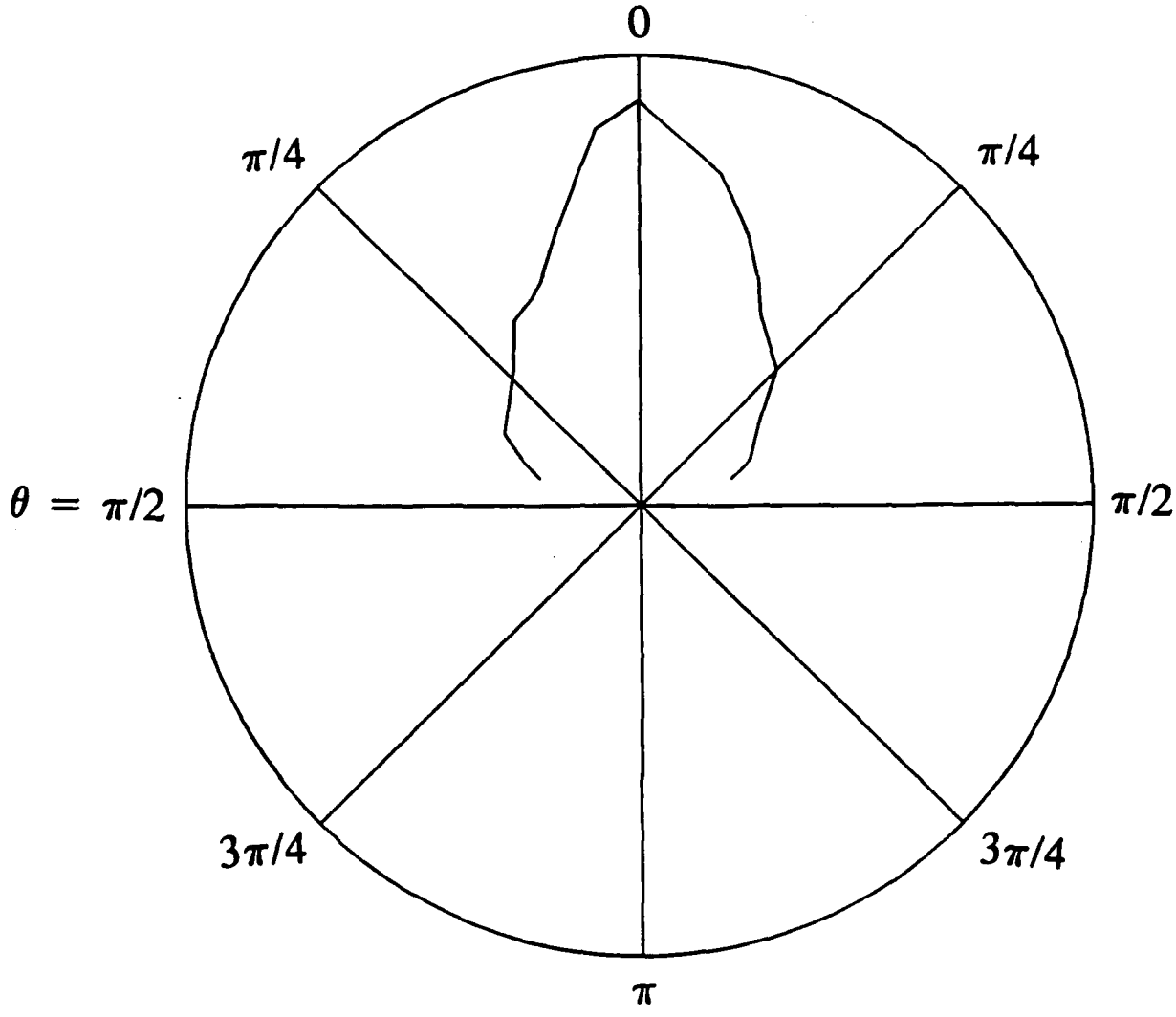

$\phi = 0$ plane: crosspolarized
(-) mode: f = 4.39 GHz
H_o = 788 Oe

Fig. 13 Radiation pattern for the (-) mode in the $\phi = 0$ plane with crosspolarized detector orientation.

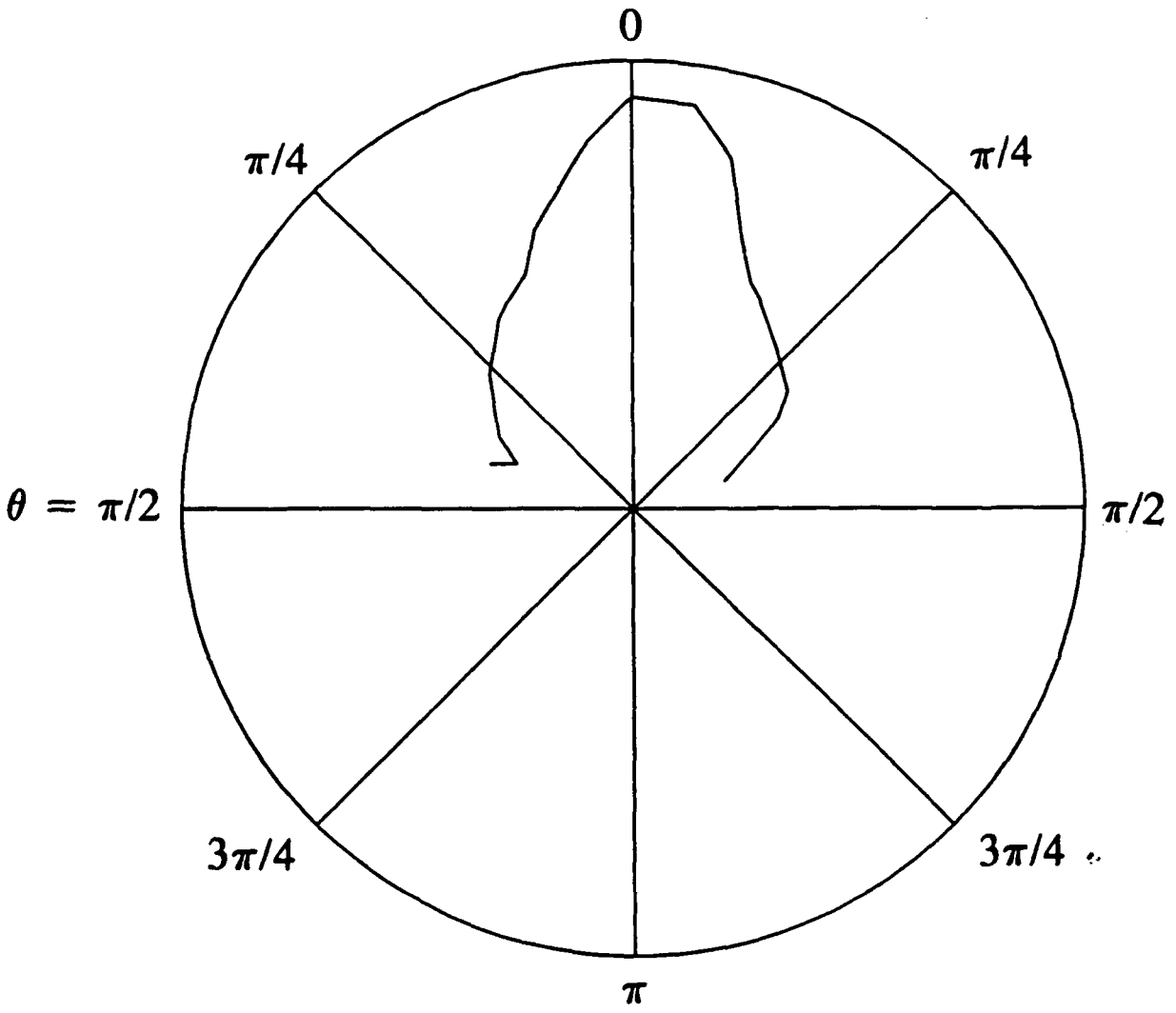

$\phi = \pi/2$ plane: copolarized
(-) mode: f = 4.39 GHz
H_o = 788 Oe

Fig. 14 Radiation pattern for the (-) mode in the $\phi = \pi/2$ plane with copolarized detector orientation.

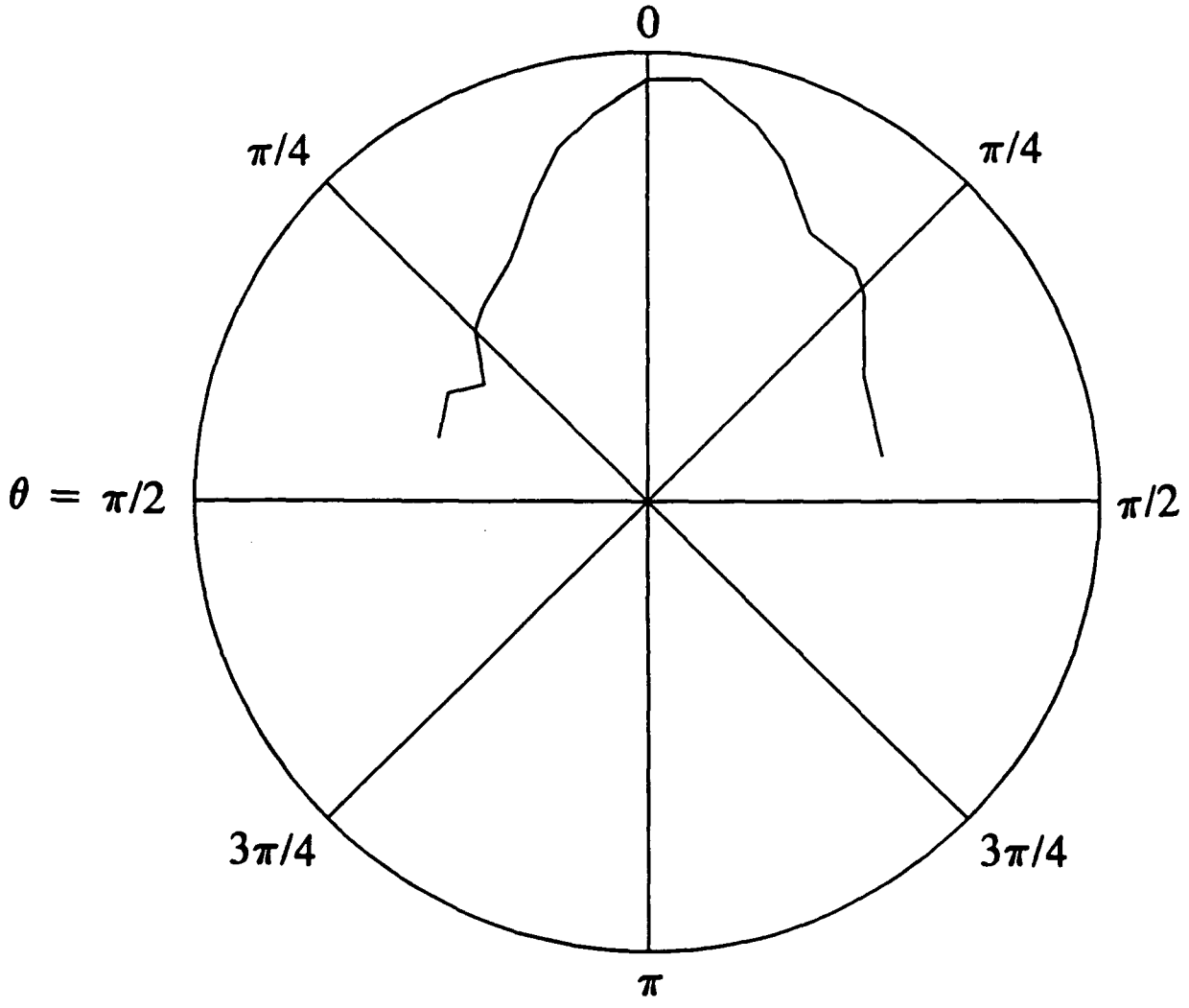

$\phi = \pi/2$ plane: crosspolarized
(-) mode: f = 4.39 GHz
H_o = 788 Oe

Fig.15 Radiation pattern for the (-) mode in the $\phi = 0$ plane with crosspolarized detector orientation.

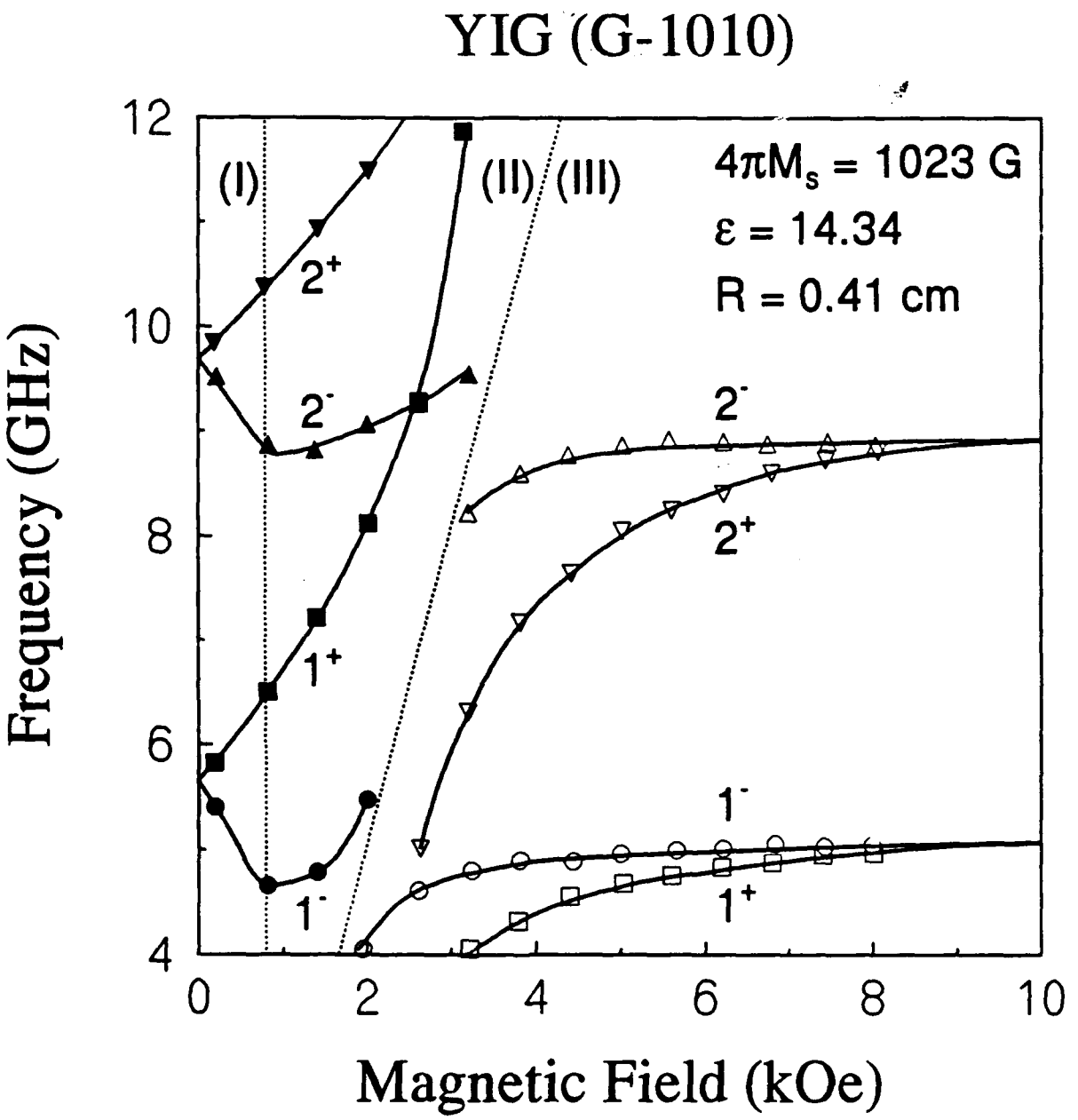

(I): Unsaturated Ferrite, (II): Biasing Below FMR

(III): Biasing Above FMR

Fig. 16 Radiation frequency as a function of the biasing field.

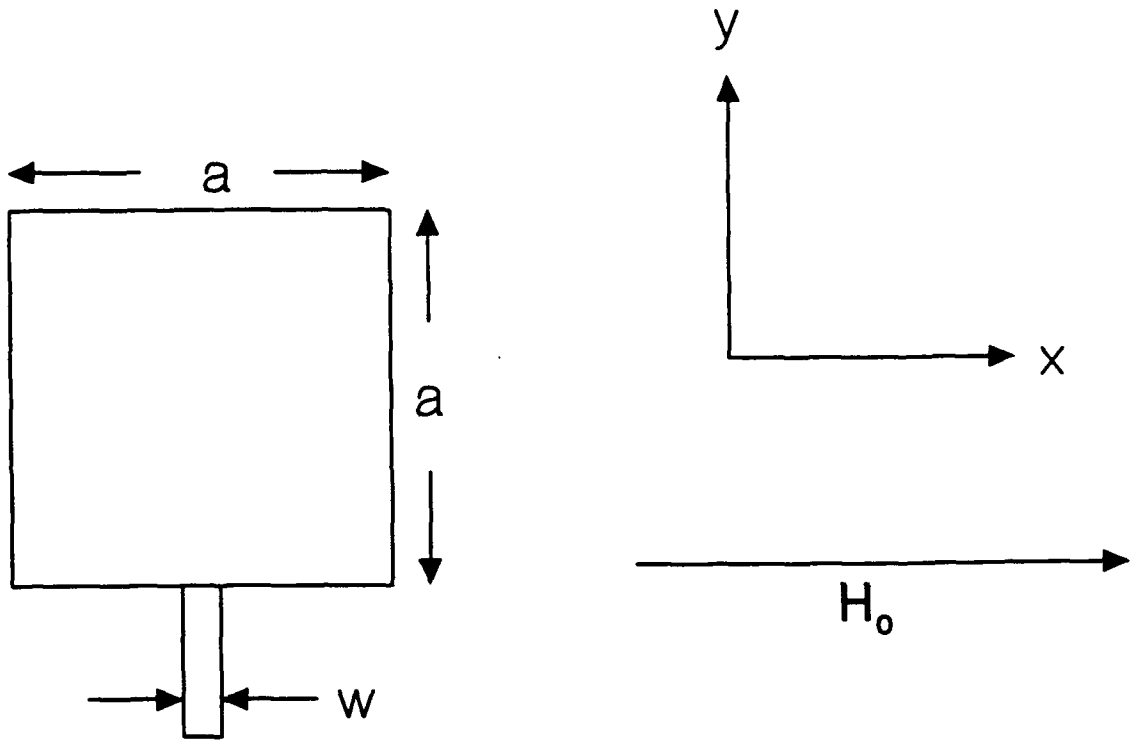

Fig.17 Schematic drawing of the microstrip antenna of square geometry.

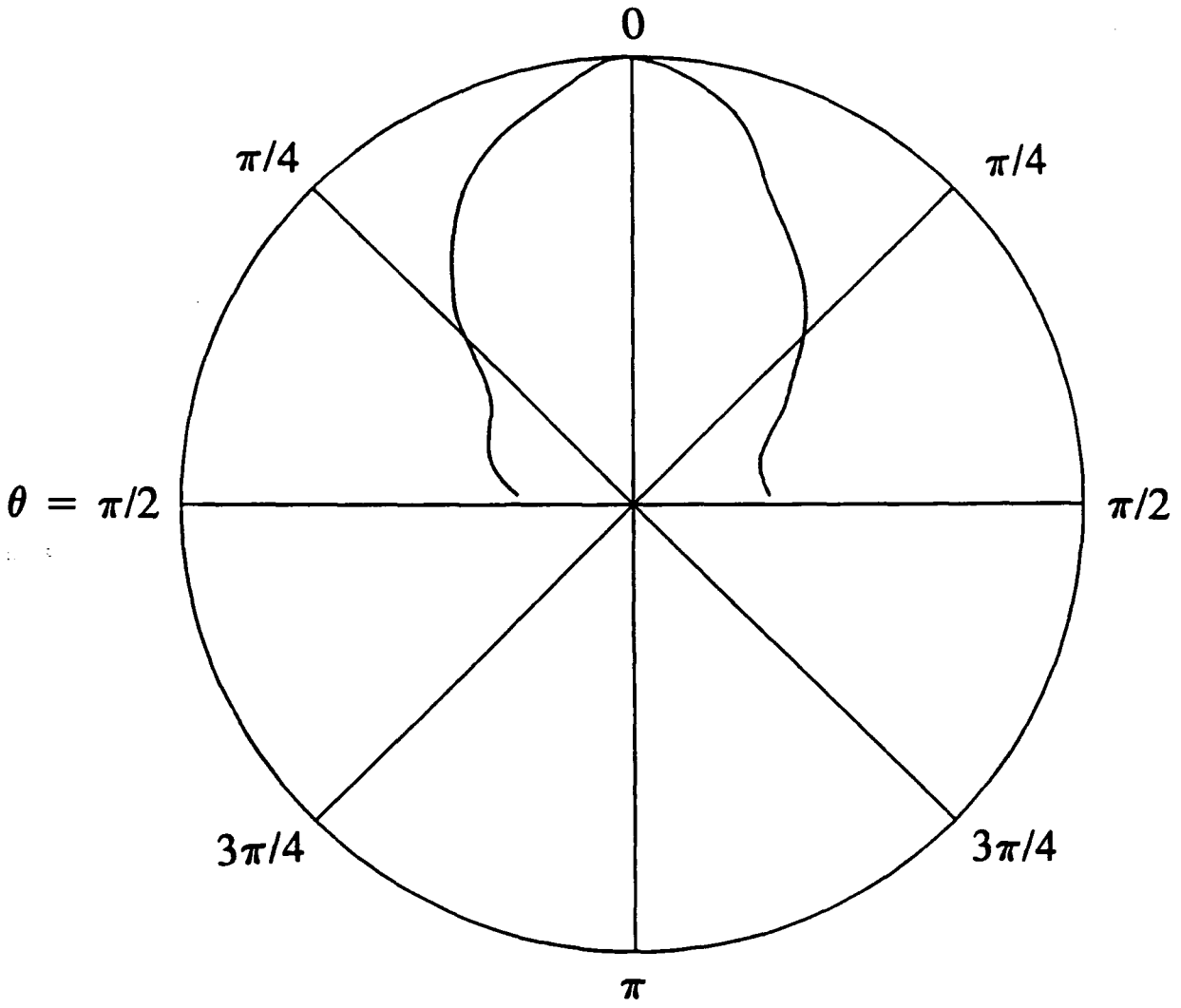

$\phi = 0$ plane: copolarized
f = 9.51 GHz, H_o = 2010 Oe.

Fig. 18 Radiation pattern of the main radiations in the $\phi = 0$ plane with copolarized detector orientation.

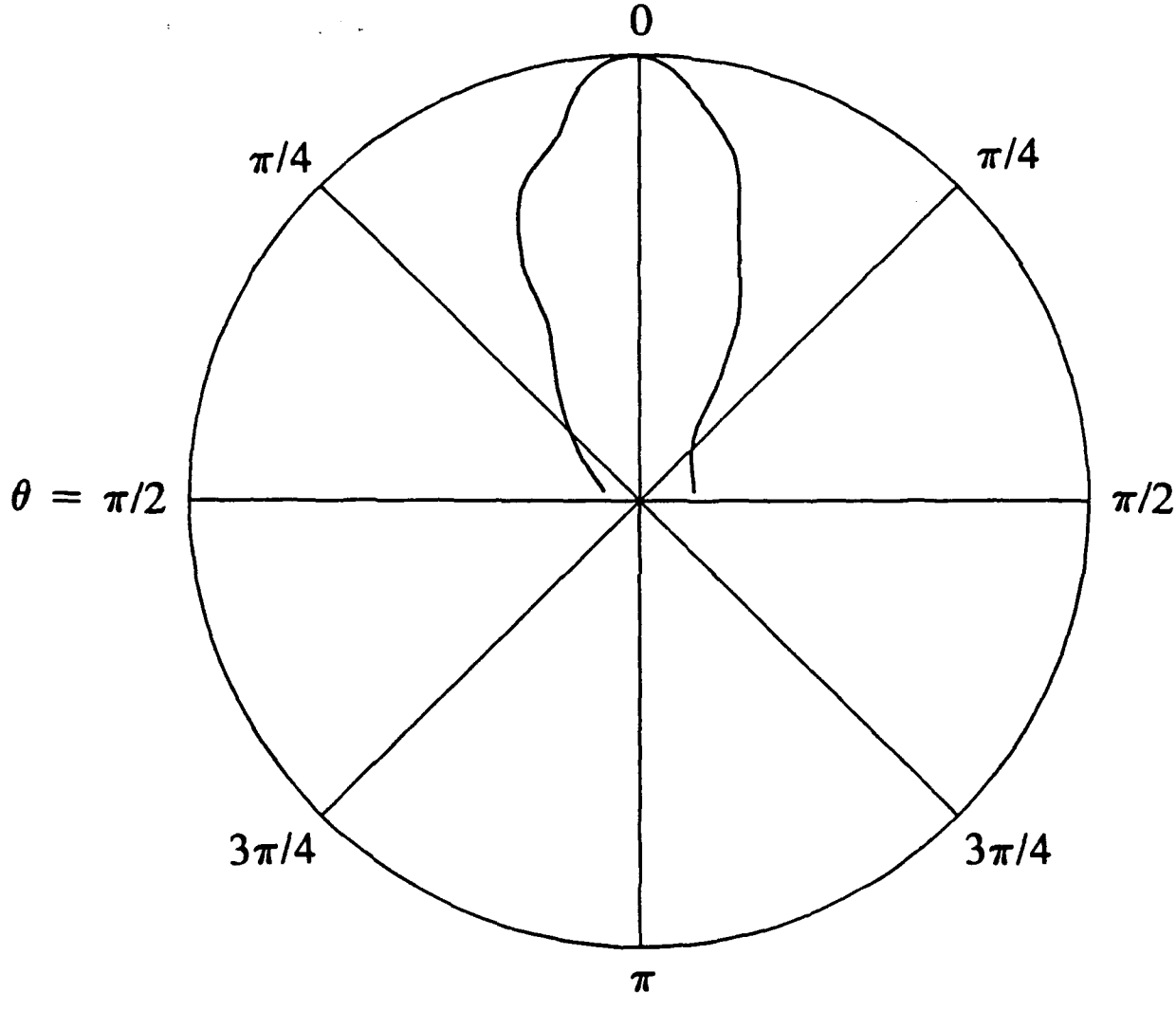

$\phi = \pi/2$ plane: crosspolarized
f = 9.51 GHz, H_o = 2010 Oe.

Fig. 19 Radiation pattern of the main radiations in the $\phi = \pi/2$ plane with crosspolarized detector orientation.

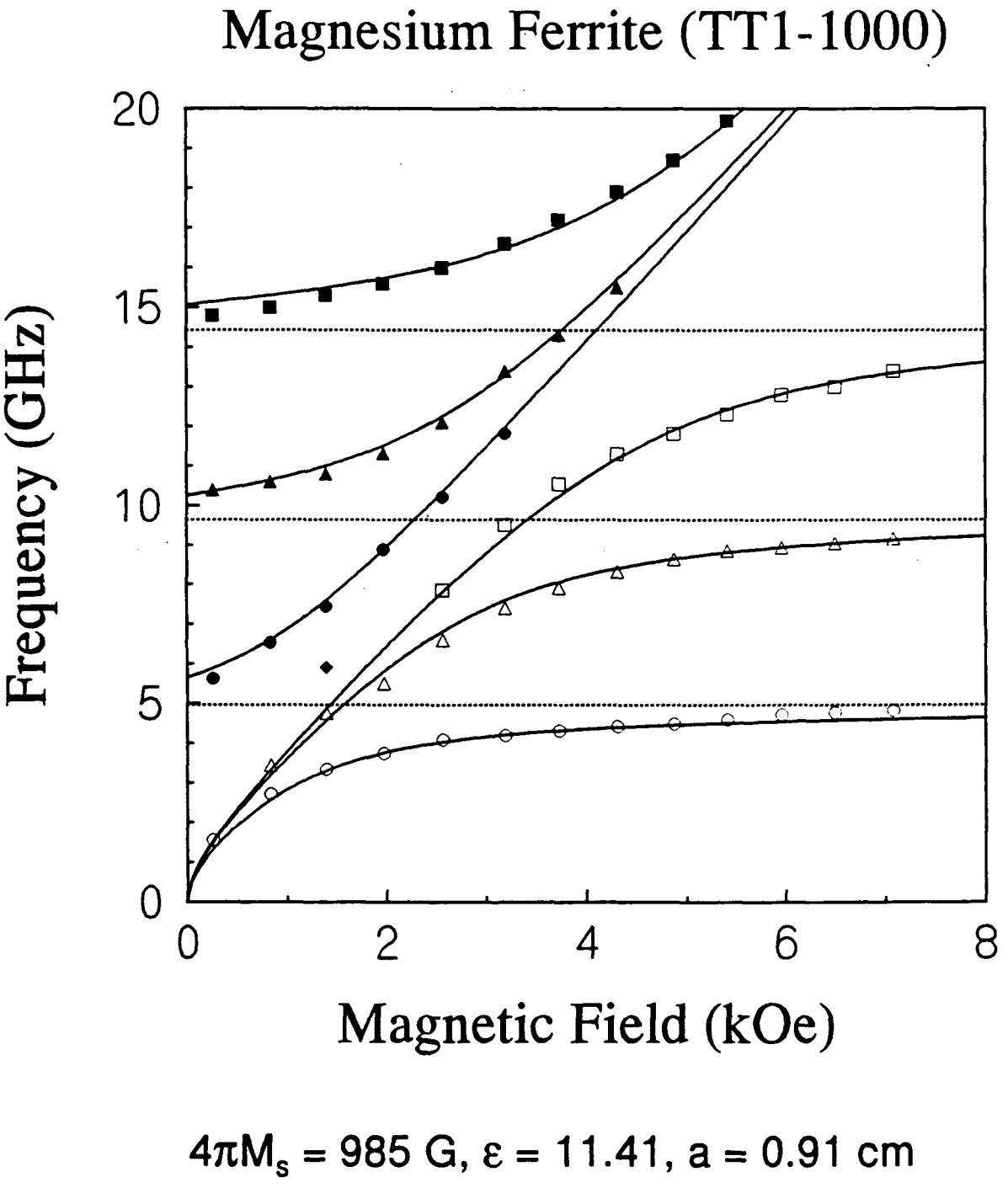

Fig.20 Radiation frequency as a function of the biasing field.

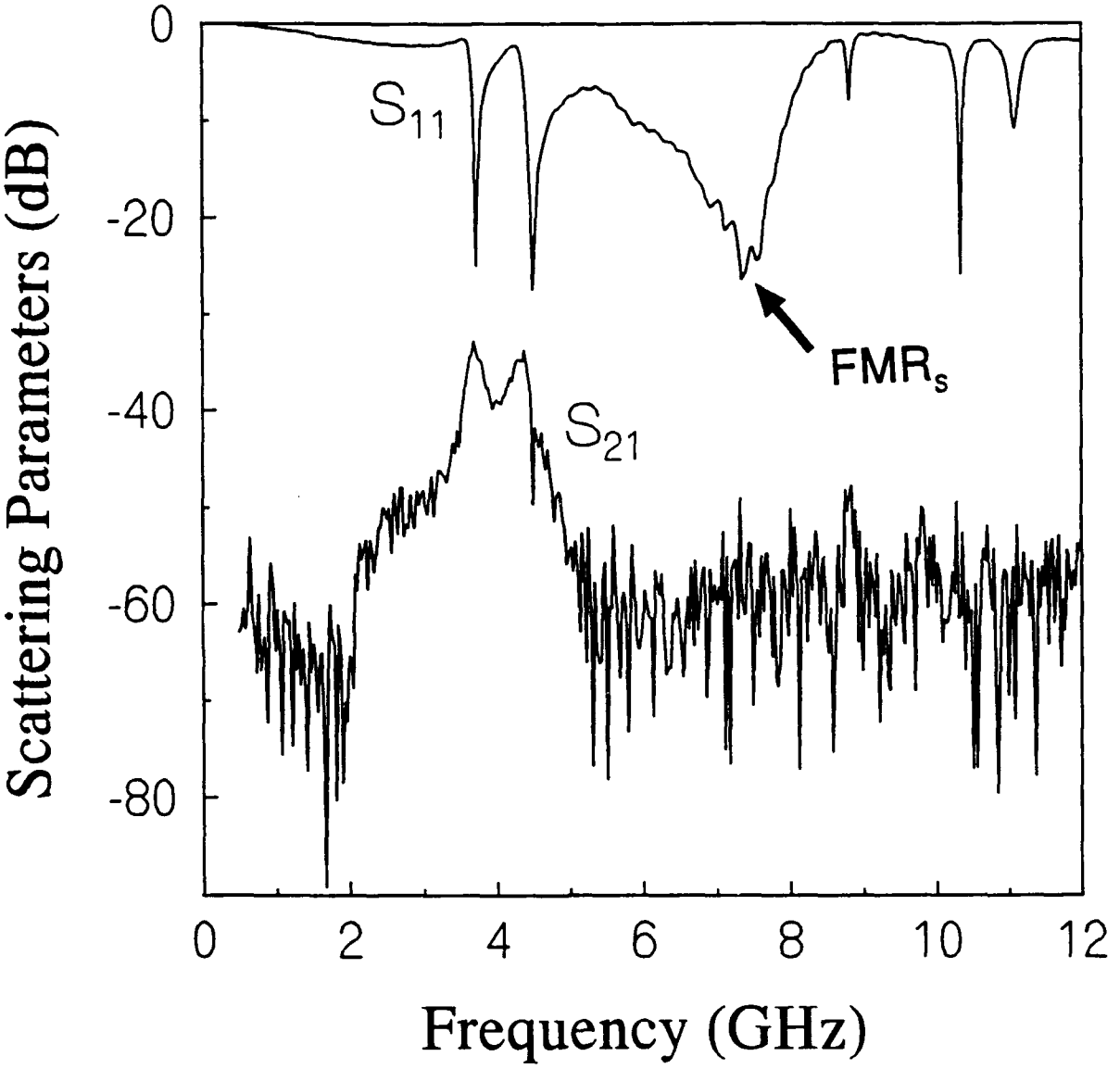

Fig. 21 Measured scattering parameters for ferrite patch antenna #2. The biasing field was 3410 Oe without covering by a top magnet disc. The detector horn antenna was oriented parallel to the microstrip feed line.

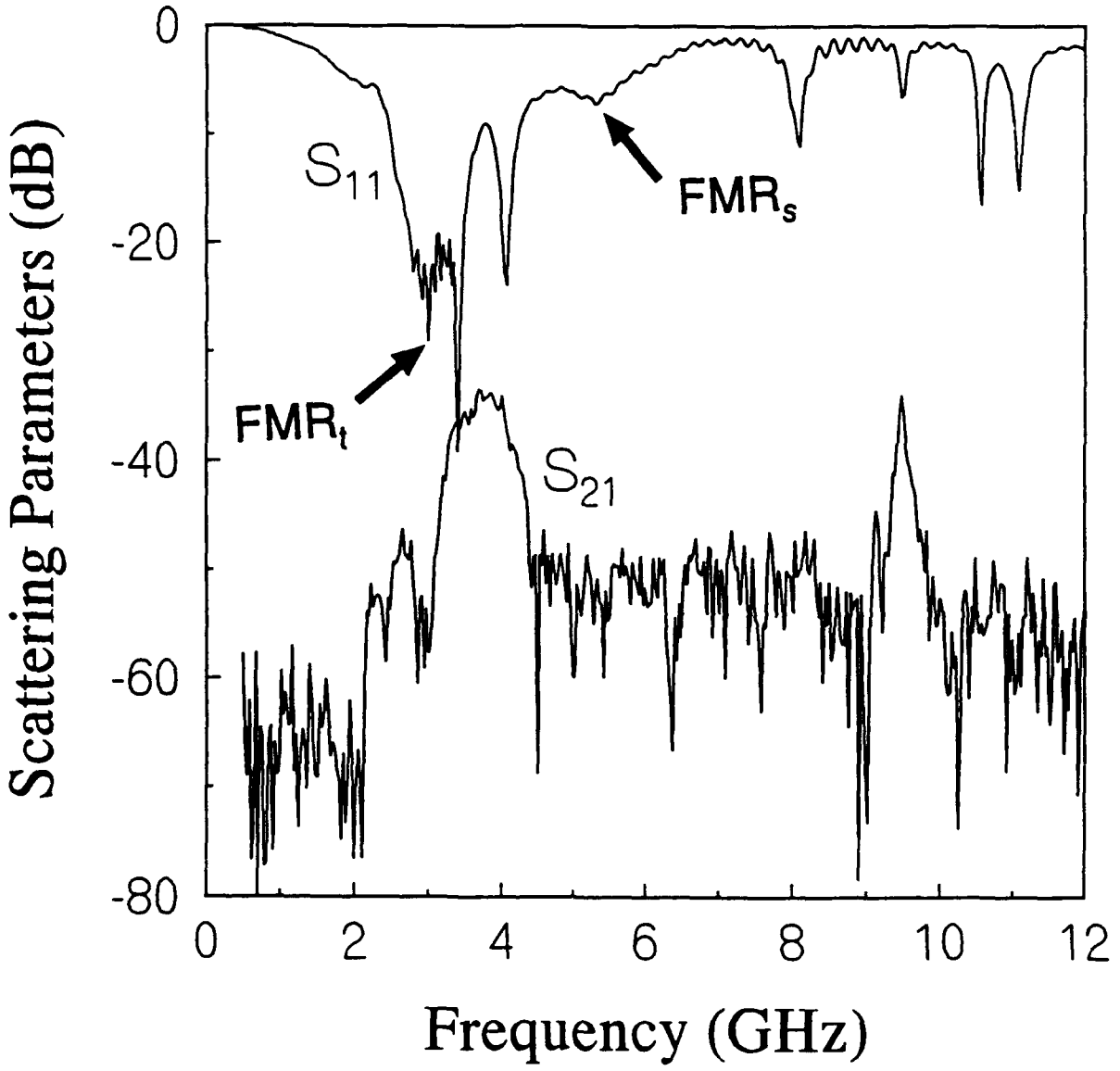

Fig. 22 Measured scattering parameters for ferrite patch antenna #2. The biasing field was 3410 Oe with covering by a top magnet disc. The detector horn antenna was oriented parallel to the microstrip feed line.

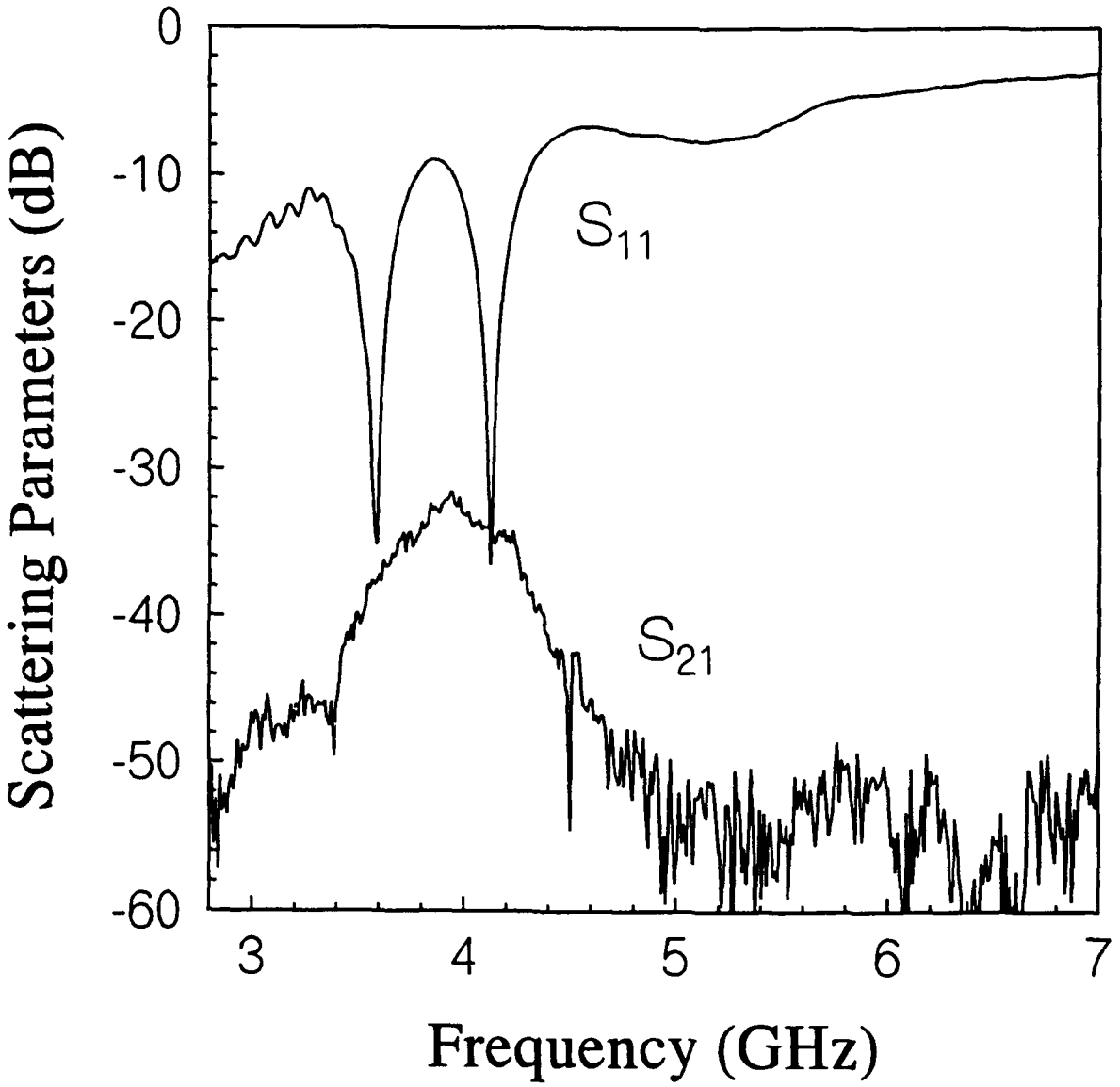

Fig. 23 Measured scattering parameters for ferrite patch antenna #2. The biasing field was 3410 Oe with covering by a top magnet disc. The detector horn antenna was oriented parallel to the microstrip feed line.

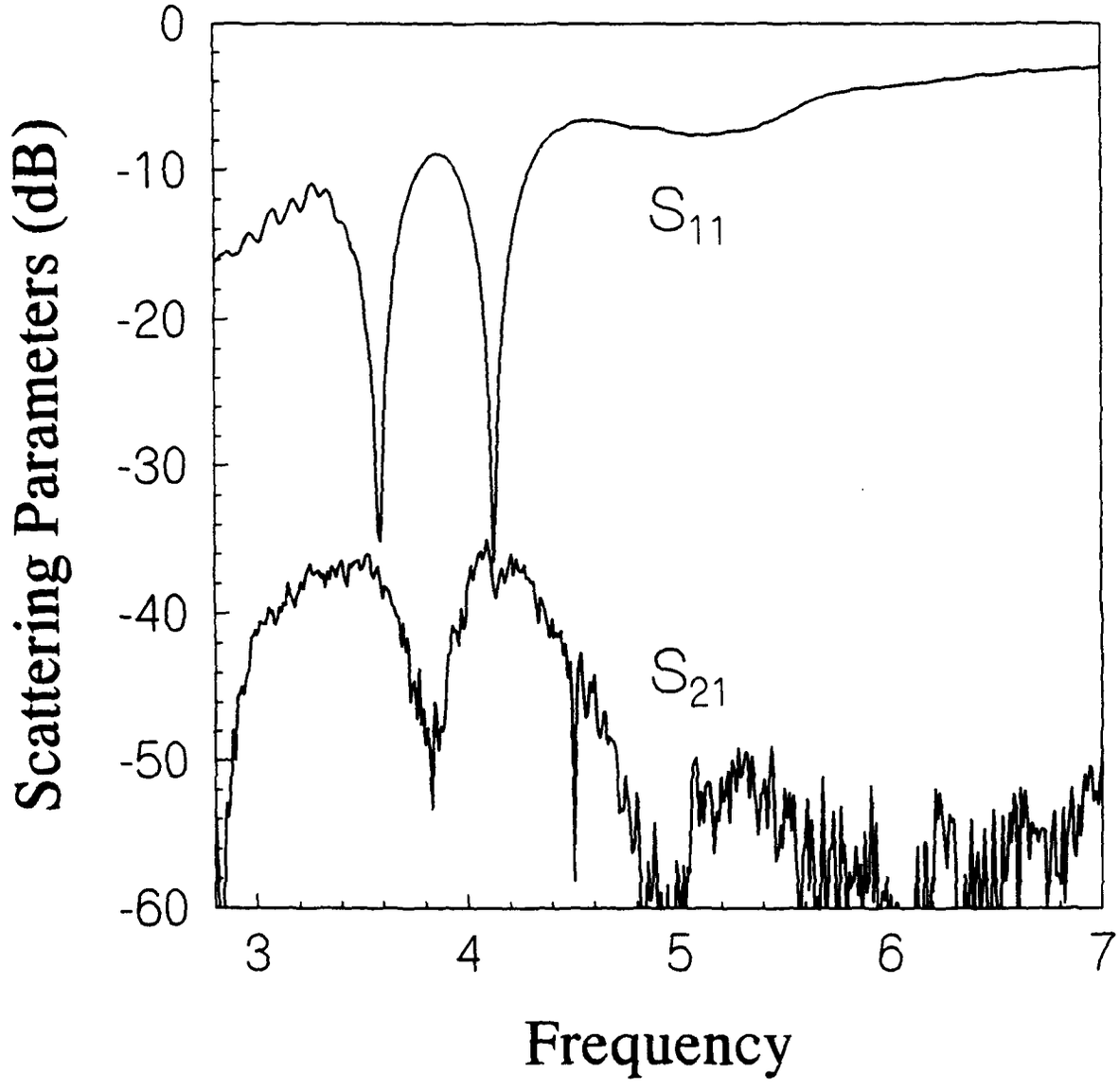

Fig. 24 Measured scattering parameters for ferrite patch antenna #2. The biasing field was 3410 Oe with covering by a top magnet disc. The detector horn antenna was oriented perpendicular to the microstrip feed line.

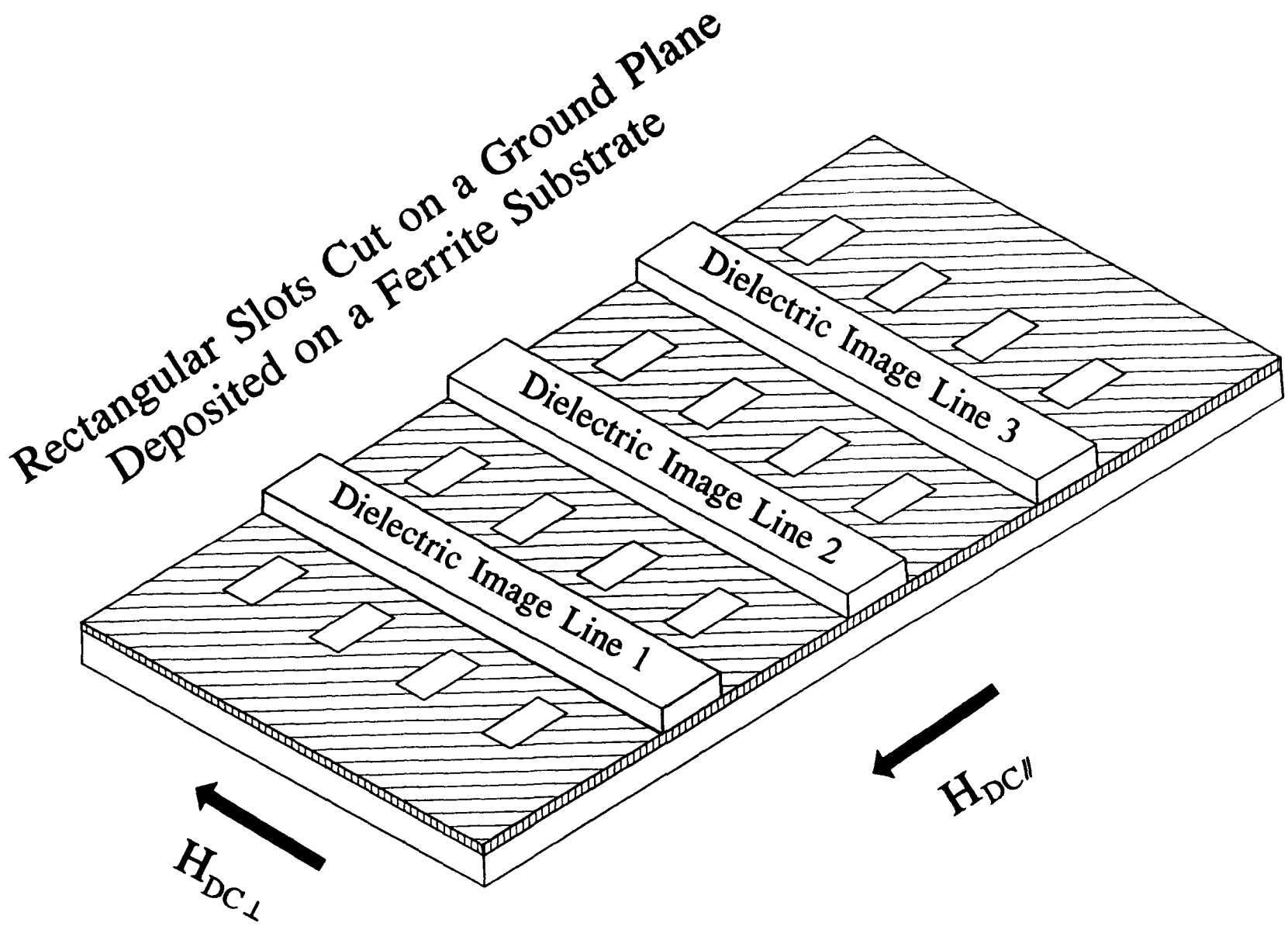

Fig. 25 Image-line feed slot antenna array used for beam steering.

Ferrite Disc Array Deployed in Front of a Waveguide Horn

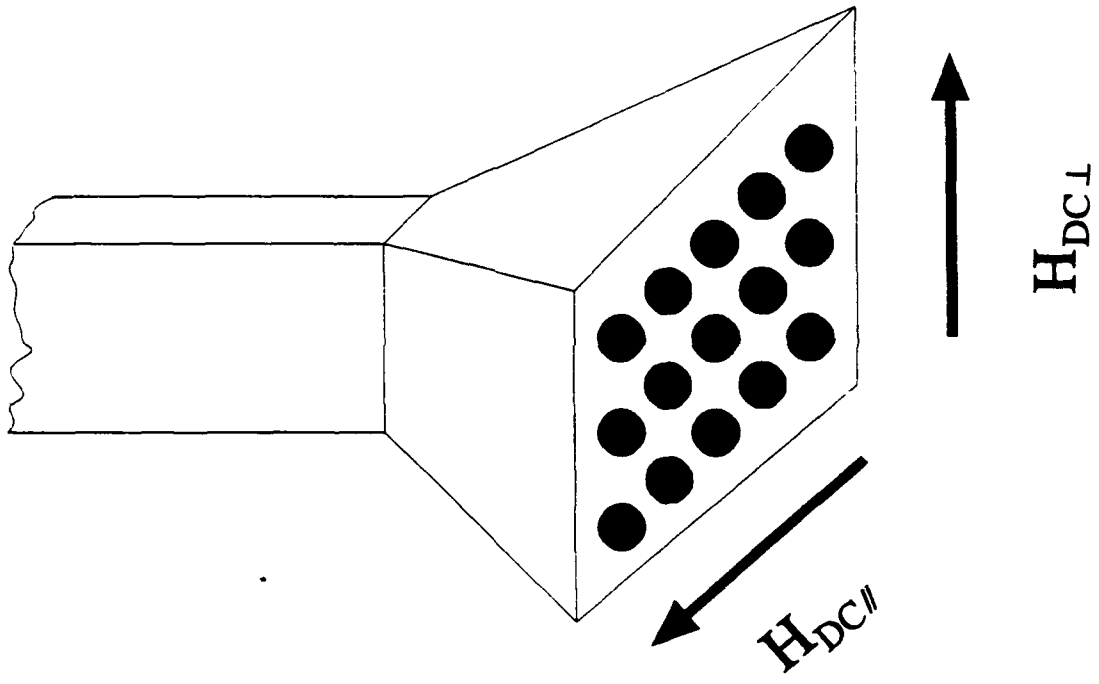

Fig. 26 Two dimensional ferrite disc scatterers used for beam steering.

XI. Appendices

Radiation Frequencies of a Microstrip Antenna on a Ferrite Substrate

H. How, D. Guan, and C. Vittoria

Department of Electrical and Computer Engineering, Northeastern University

Boston, MA 02115

Abstract - We have formulated and experimentally confirmed two types of radiation modes for patch antennas loaded with ferrite materials. Each type of radiation is a linear conbination of normal modes of propagation in an unbounded medium consisting of parallel plate separated by a slab of ferrite material. Ferrite patch antennas of square geometry have been fabricated and tested. The measured resonant frequencies of these new modes of radiation compared very well with our theory.

Introduction

In the past we have reported on a theory which calculated the normal mode frequencies of a microstrip patch antenna on a "magnetically unsaturated" ferrite substrate.[1] In this paper we have extended the theory to patch antennas consisting of ferrite substrates which are magnetically saturated. Specifically, we have formulated the ferrite patch antenna problem in terms of the so-called cavity model.[2] The cavity is physically bounded by electric walls at the top and bottom of the patch antenna. However, the boundary conditions at the periphery (side wall) of the patch antenna require the Poynting vector to vanish. Energy is confined within the cavity and in this manner radiation frequencies can be readily calculated. We found that only TE modes of oscillations exist in the patch antenna cavity. These TE modes are distinguished as transverse modes and longitudinal modes relative to the magnetization direction, $\vec{M}$. For example, for TE mode of propagation perpendicular/parallel to $\vec{M}$ we identify this as transverse/longitudinal TE mode. While the longitudinal TE modes are found to form discrete modes in the frequency domain, the radiation frequency of a transverse TE mode can be continuously tuned over a wide frequency range by varying the biasing magnetic field. Measurements of the radiation frequencies of square ferrite patch antennas deposited on substrates of magnesium ferrite have been made and they compared very well with our theory.

Fig.1 shows the geometry of a microstrip patch antenna of square geometry. The length of the square patch is a and a microstrip line of width w is fed into the antenna at the center of one side of the patch. The metal patch is deposited on a ferrite substrate whose thickness, dielectric constant, and saturation magnetization are denoted as d, ϵ, and $4\pi M_s$, respectively. The

external field, H_o, is applied along the edge of one side of the patch and perpendicular to the microstrip feed line. The coordinates used for describing the patch antenna are shown in Fig.1. Procedures for solving the intrinsic modes of radiation frequencies in a ferrite patch antenna are as follows: we first construct the propagtion modes in a parallel plate waveguide loaded with a ferrite slab of thickness d. The top square patch of the antenna is temporarily replaced by an infinite conducting sheet. The normal mode solutions of the finite ferrite cavity can be then composed as superpositions of the propagation modes of the waveguide, provided that boundary conditions are satisfied at the periphery of the cavity. For dielectric patches one normally assumes magnetic wall boundary conditions at the patch periphery.[2] However, for a ferrite patch antenna magnetic wall boundary conditions can not give rise to proper solution of the radiation frequencies, since this boundary condition gives rise to trivial solutions in which the electromagnetic fields vanish everywhere in the cavity. We suggest in this paper the use of the so-called "insulation wall" boundary condition. We define an insulation wall to be the conditions at which no electromagnetic energy can flow across the wall. This implies that the normal component of the Poynting vector vanishes at an insulation wall. We note that an electric wall or a magnetic wall is an insulation wall, but an insulation wall is not necessarily an electric wall or a magnetic wall.

A full derivation of the normal mode solutions within a ferrite cavity is beyond the scope of the present paper and will be published elsewhere.[3] In this paper we summarize the properties of the normal mode solutions of the radiation frequencies which are compared with experimental data. One may distinguish three types of normal modes. The first type is the dielctric or

the uncoupled mode. For the uncoupled mode the rf h-field is parallel to the dc applied field which are both perpendicular to the wave propagation direction of that mode. As such, there is no magnetic coupling and the effective permeability value is 1. For the second type of normal mode, or the so-called Voigt mode, the rf h-field, the dc magnetic field, and the propagation direction are all perpendicular to each other. The Voigt modes are therefore referred to as the transverse TE modes. The Voigt permeability is given by[3]

$$\mu_v = 1 + 4\pi M_s(4\pi M_s + H_o)/(H_o^2 + 4\pi M_s H_o - f^2/\gamma^2), \qquad (1)$$

where f is the frequency and γ denotes the gyromagnetic ratio. Voigt modes are continuous modes, since the normal mode frequencies can be continuously tuned by varying the external biasing magnetic field, H_o.

The third type of normal modes are longitudinal TE modes whose propagation direction is along the dc field. Longitudinal TE modes form dicrete modes (subject to no frequency-tuning capability) and require nodal points in the z-direction. This is in contrast to the former two types of normal modes which assume no field variation along the z-direction. Formation of longitudinal TE modes is similar to the internal reflection of electromagnetic waves in a birefringent medium; the ordinary and the extraordinary waves form standing waves in the z-direction involving differnent number of nodal points. The longitudinal TE modes appear near the region of ferrimagnetic resonance (FMR). We note that all of the three types of normal modes result in linearly polarized radiations in the far zone. The polarization axis of a Voigt-mode is orthogonal to that associated with the other two types of normal mode radiations.

We have fabricated a square patch antenna using magnesium-ferrite substrate, TT1-1000 (Trans-Teck, MD, USA). The substrate is of dimension 0.02" × 2" × 2", and the patch is 3/8" × 3/8". A microstrip line of width 0.43 mm is used as the feed line. The antenna was inserted in an electromagnet which provided magnetic fields up to 9 kOe. S_{11} data were taken using a network analyzer (HP8510B) which was connected to an HP computer. Fig.2 shows the measured resonant frequencies of the patch antenna as a function of the applied magnetic field. In Fig.2 full dots represent biasing-below-FMR data, and open dots above FMR. The dashed lines are purely dielectric or uncoupled modes whose frequencies are independent of the applied field. The intensities as measured in changes in S_{11} of the dielectric or uncoupled modes were very weak compared to the ferrite or coupled modes. The uncoupled modes were observed mostly for magnetic fields below FMR. The solid lines in Fig.2 are theoretical curves for the Voigt modes calculated from Eq.(1) using the following parameters: $4\pi M_s$ = 985 G, ϵ = 11.41, and a = 0.91 cm. The $4\pi M_s$ and ϵ values are furnished by the manufacturer, and the patch dimension, a, is determined by a best-fit algorithm, since the physical dimension of the patch (3/8" = 0.953 cm) does not imply the dimension of the embedded cavity resonator. A discrete data point, solid diamond, is also shown in the near-FMR region of Fig.2 reminiscent of the longitudinal TE mode. Since the longitudinal TE mode exhibited very low intensity, other high-order longitudinal TE modes were not observed in the present S_{11} measurements. In Fig.2 the agreement between theory and experiments is good.

In order to measure the radiation pattern of the ferrite patch antenna we have used permanent magnets in biasing the ferrite substrate. Two permanent neodymium magnet discs of diameter 0.5" and height 0.19" were arranged face-

neodymium magnet discs of diameter 0.5" and height 0.19" were arranged face-to-face directly below the ferrite substrate (beneath the ground plane). This produces transverse magnetic field for the substrate in the order of 2 kOe. Figs.3a and 3b show the radiation profiles in the principal planes for a Voigt mode (f = 9.51 GHz, $H_o \approx$ 2010 Oe). Main radiations are copolarized in the $\phi = 0$ plane and crosspolarized in the $\phi = \pi/2$ plane. Other polarizations were about 10 dB below the main radiations. This verifies the tansverse nature of the Voigt modes. We have also measured similar radiation patterns for the dielectric mode (f = 4.93 GHz) and the longitudinal TE mode (f = 5.91 GHz, $f_o \approx$ 1470 Oe). However, the polarization patterns were rotated 90^o away from those of Figs.3a and 3b, and the measured intesities were about 10 dB lower than the main radiations of the Voigt modes.

We conclude that Voigt modes might have potentials for important engineering applications. For example, Fig.2 shows the possibility for wideband frequency tuning capability involving single mode operation. That is, the fundamental mode for biasing-below-FMR can be roughly single-mode-tuned from 5 to 10 GHz by varying the field from 0 to 2.5 kOe.

References

1. H. How, P. Rainville, F. Harackiewicz, and C. Vittoria, "Radiation Frequencies of Ferrite Patch Antennas", Electronics Letters, Vol.28 (15), p.1405 (1992).
2. Y.T. Lo, D. Solomon, and W.F. Richards, "Theory and Experiment on Microstrip Antenna Element", IEEE Trans. MTT-27, p.137 (1979).
3. H. How and C. Vittoria, "Intrinsic Modes of Radiation in Ferrite Patch Antennas", to be published.

Figure Captions

Fig.1 Schematic drawing of the microstrip antenna of square geometry.

Fig.2 Measure resonant frequencies of a square ferrite patch antenna.

Fig.3 Measured radiation patterns in the $\phi = 0$ and $\pi/2$ planes.

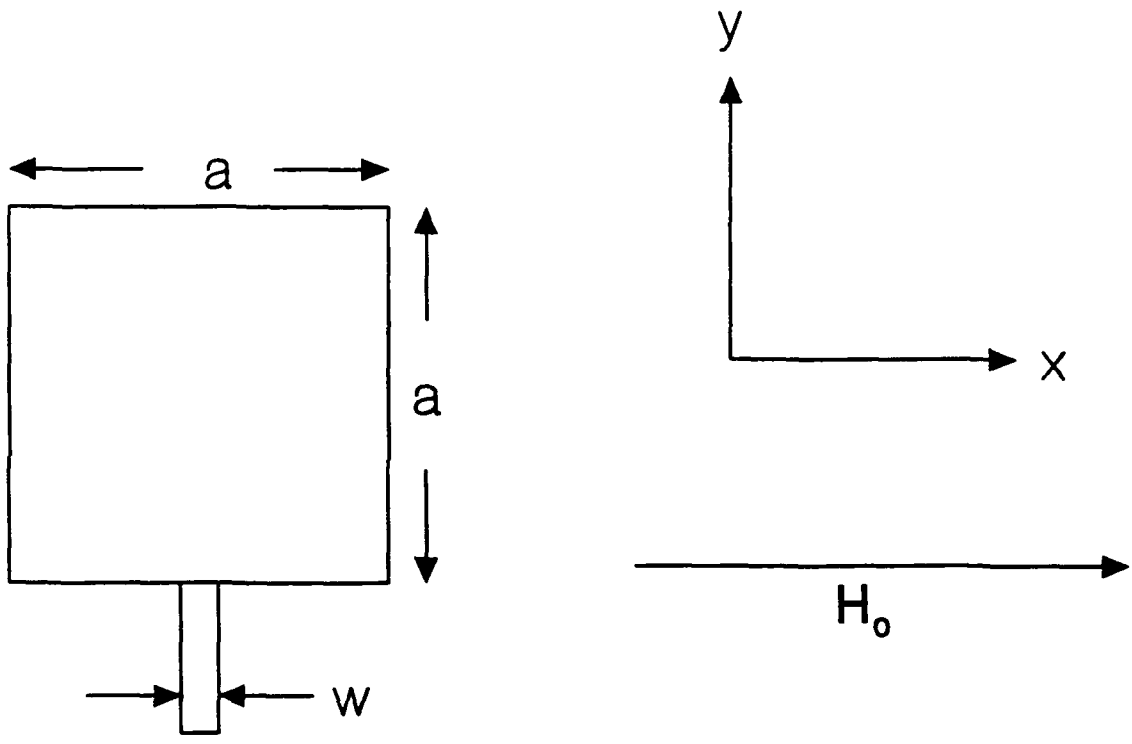
a
a
w
y
x
H_o

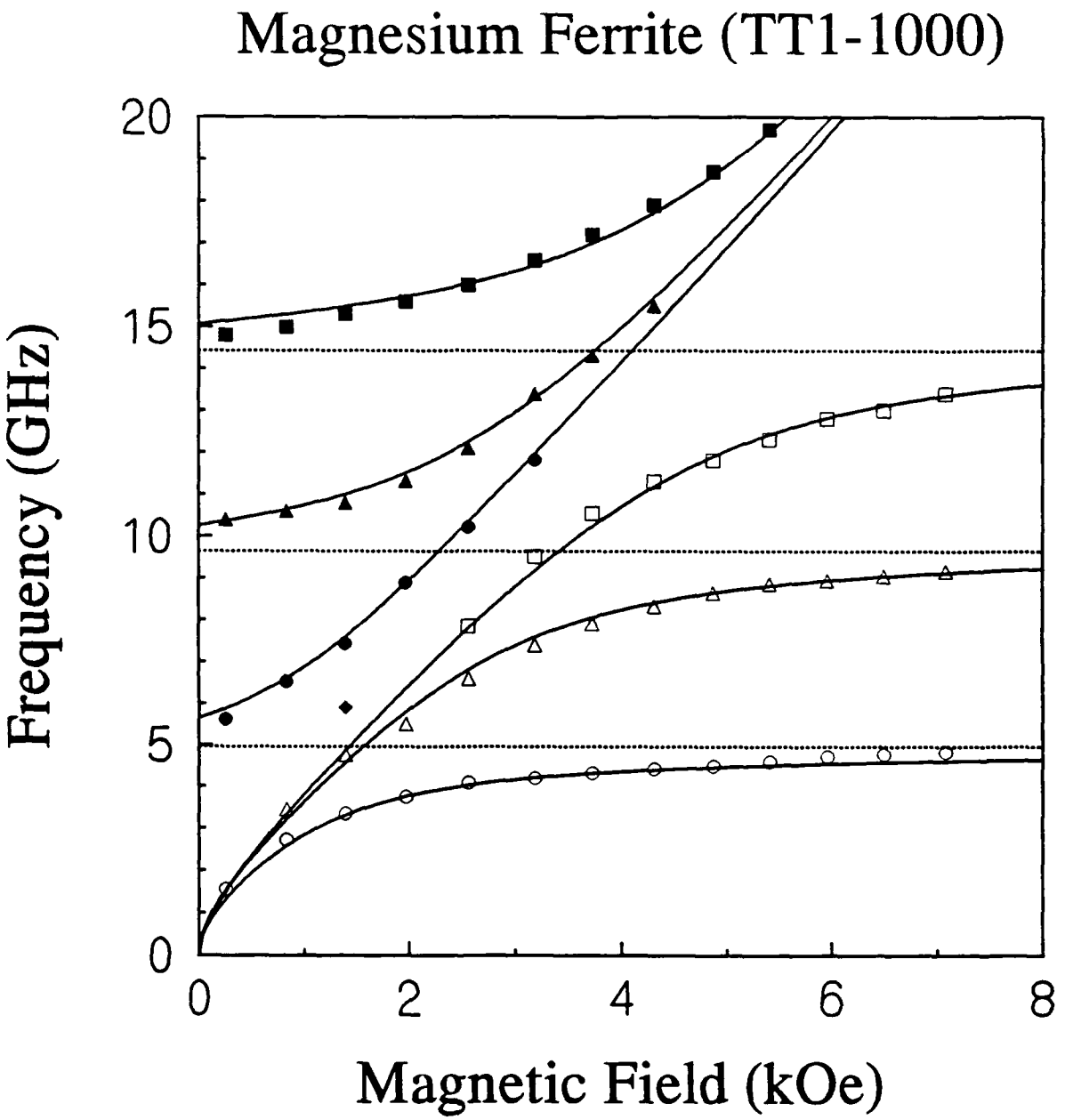

$4\pi M_s$ = 985 G, ε = 11.41, a = 0.91 cm

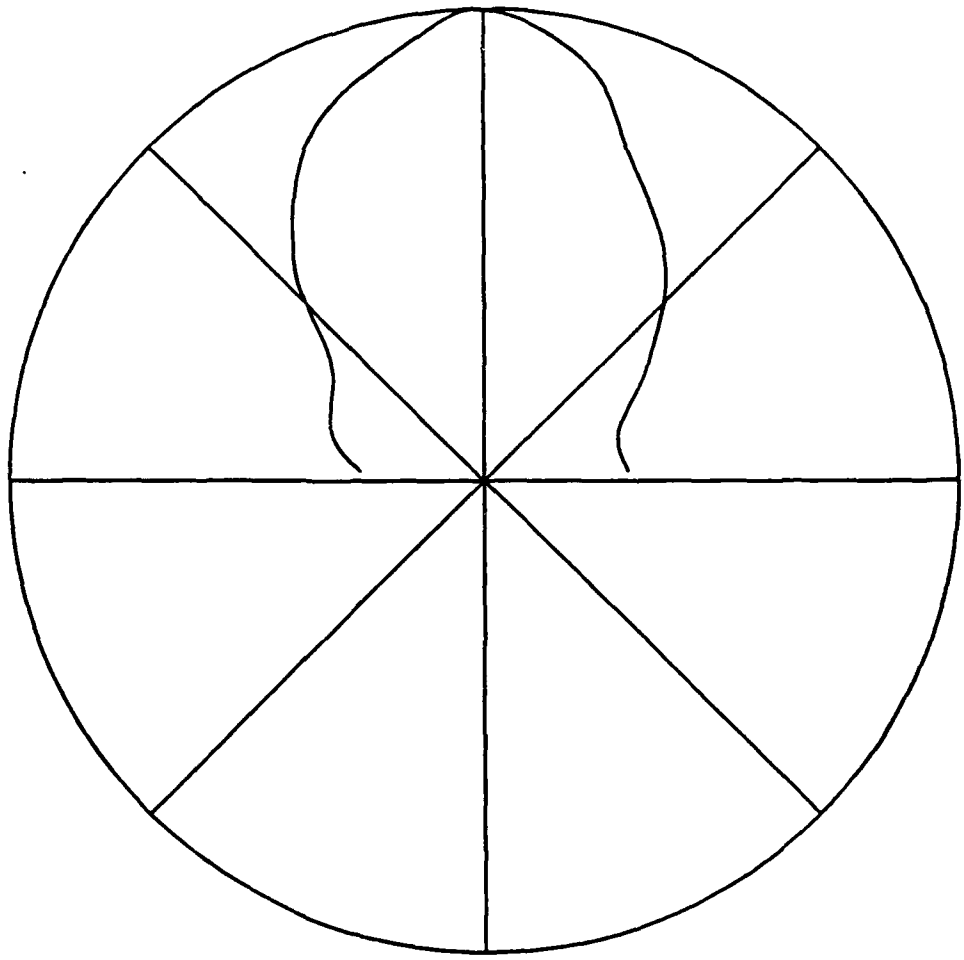

ϕ=0 plane: copolarized

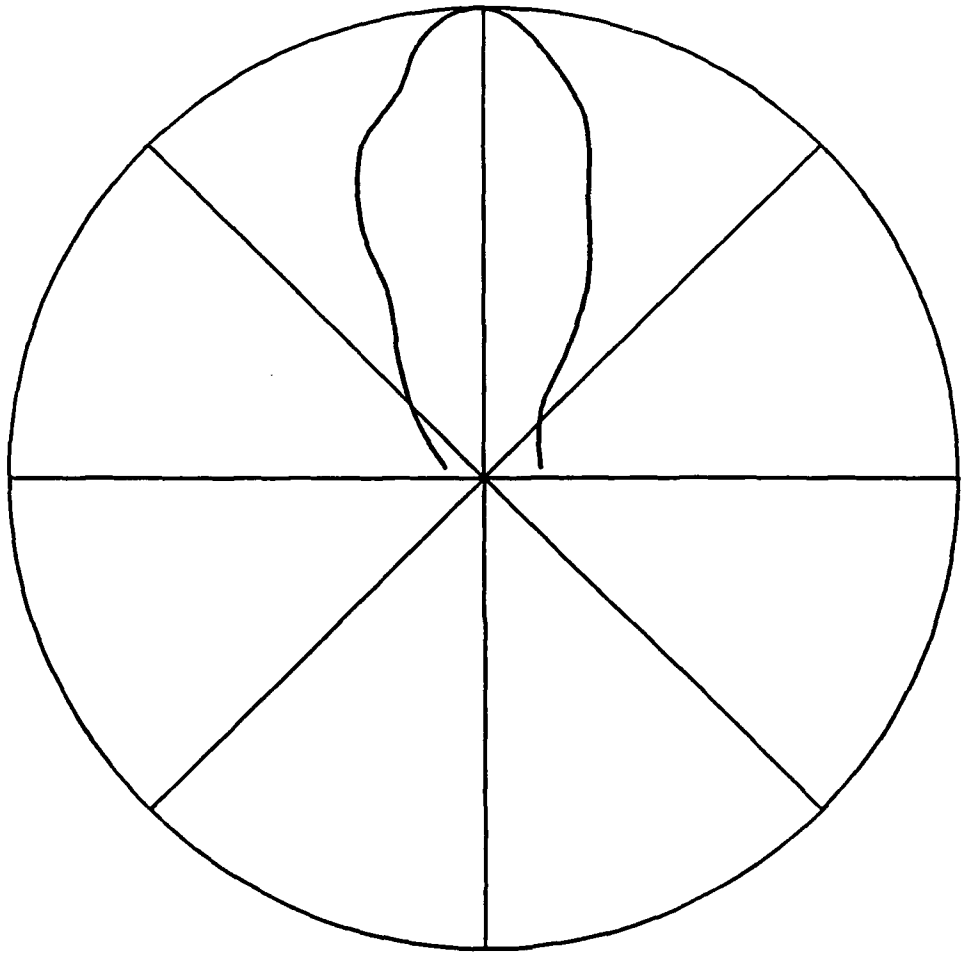

$\phi=\pi/2$ plane: crosspolarized

Instrinsic Modes of Radiation in Ferrite Patch Antennas

H. How and C. Vittoria

Electrical and Computer Engineering Department, Northeastern University

Boston, MA 02115

Abstract - We have found two types of radiation modes for patch antennas loaded with ferrite materials. Each mode of radiation is a linear conbination of normal modes of propagation in parallel plate waveguide separated by a slab of ferrite material. We have introduced new boundary conditions in which only TE modes of oscillation in the patch antenna cavity result. According to different propagation directions relative to the applied dc field these TE modes are distinguished as transverse modes and longitudinal modes, and they possess mutually perpendicular radiation polarizations. While the longitudinal TE modes are found to form discrete modes in the frequency domain, the radiation frequency of a transverse TE mode can be continuously tuned over a wide frequency range by varying the biasing magnetic field. Circularly polarized radiations may result from simultaneous excitations of these two modes. Ferrite patch antennas of square geometry have been fabricated and tested. The measured resonant frequencies compared very well with our theory.

Introduction

The microwave applications of ferrites had their foundation in the early work of the Faraday effects. Polder[1] derived the tensor permeability of the ferrite media, and Suhl and Walker[2] solved the problem of circular waveguide filled with longitudinally magnetized ferrite. Unz[3] discussed the solutions of the propagation waves in a generally magnetized ferrite filled between two conducting parallel planes. We consider in this paper the resonating modes of a ferrite patch antenna. Ferrite patch antennas consist of metallic patches deposited on ferrite substrates. The substrates are electrically grounded by placing them on a metal surface. Recently there has been great interest in developing ferrites in patch antenna designs in order to incorporate phase shiftering, impedance matching, frequency tuning, and nonreciprocal effects in the operation of antennas. It has been reported that by including ferrite materials the main beam from an antenna array can be scaned,[4] and the radiation frequency of a microstrip antenna can be tuned by varying the biasing magnetic field.[5] We are exploring another application of ferrite patch antennas and that is the radiation of circularly polarized electromagnetic waves. Conventional circularly polarized patch antennas are designed on the basis of single-fed elliptic patches or dual-fed rectangular patches. For single-fed elliptic patches the amount of ellipticity of the patch geometry controls the mixing of the two orthogonal linearly-polarized radiations, which in turn gives rise to the circularly polarized waves.[6] For dual-fed rectangular patches two orthogonal feeds are required in which the relative phases are shifted 90^{o} apart from each other.[7] A ferrite patch antenna can excite radiation patterns of spatially cross linear polarizations, and hence provide a third possibility for designing

circularly-polarized antennas.

We have developed in this paper an analytic expression for the resonating fields excited in a ferrite patch antenna cavity. We have formulated the ferrite patch antenna problem in terms of the so-called cavity model.[8] The cavity is physically bounded by electric walls at the top and bottom of the patch antenna. However, we have modified the boundary conditions of the cavity model at the perophery (side wall) of the patch attenna. In our application we require the Poynting vector to vanish at the periphery instead of the normally applied magnetic wall boundary conditions. Energy is confined within the cavity and in this manner radiation frequencies as well as radiation patterns can be readily calculated. The input impedance and bandwidth of a patch antenna can also be estimated using this modified cavity model if the perfect wall conditions are relaxed to allow for fringe field effects.[9] Measurements on square ferrite patch antennas deposited on substrates of magnesium ferrite are reported which compared very well with our theory.

Calculations

I. Guiding modes in parallel plate waveguide

Consider a parallel plate waveguide filled with ferrimagnetic material. Results for the propagation of electromagnetic waves in a bulk ferrite are summarized in the Appendix.[10] Let the dc bias field be applied parallel to the conductor planes located at $z = 0$ and $z = d$. For other applied field directions the reader is refered to Ref.3 where more general solutions were found for a ferrite parallel plate waveguide (utilizing the operational calculaus method). In the present case the metal boundary conditions require

b_z, e_x, and e_y to vanish on the metal surfaces. We consider the following three cases.

(1) Uncoupled case

In this case $\vec{h} \parallel \vec{H}_{in} \perp \vec{k}$ and no magnetic coupling is possible. This reduces to the regular isotropic case ($\mu_e = 1$) and hence no further discussion will be made for this case.

(2) Voigt configuration

In this case $\vec{h} \perp \vec{H}_{in} \perp \vec{k}$ and

$$\mu_e = 1 + \frac{\omega_m(\omega_m + \omega_o)}{\omega_o^2 + \omega_m\omega_o - \omega^2} . \tag{1}$$

The guiding wave solutions may be expressed as

$$e_x = E_o \exp(-jk_2y) \sin(k_3z), \tag{2a}$$

$$e_y = 0, \tag{2b}$$

$$e_z = 0, \tag{2c}$$

$$h_x = 0, \tag{3a}$$

$$h_y = \frac{E_o}{j\zeta} \exp(-jk_2y) \, \mathrm{Re}\left[\frac{\alpha_2\alpha_3\mu_e\omega j + (1 - \alpha_2^2\mu_e)\omega_o + \omega_m}{(\omega_o + \omega_m)\alpha_3 + \alpha_2\omega j} \exp(-jk_3z)\right], \tag{3b}$$

$$h_z = \frac{E_o}{\zeta} \exp(-jk_2y) \, \mathrm{Im}\left[\frac{-(1 - \alpha_3^2\mu_e)\omega j - \alpha_2\alpha_3\mu_e\omega_o}{(\omega_o + \omega_m)\alpha_3 + \alpha_2\omega j} \exp(-jk_3z)\right], \tag{3c}$$

$$b_x = 0, \tag{4a}$$

$$b_y = \frac{\alpha_3\mu_o\mu_e E_o}{j\,\zeta} \exp(-jk_2y) \cos(k_3z), \tag{4b}$$

$$b_z = \frac{-\alpha_2\mu_o\mu_e E_o}{\zeta} \exp(-jk_2y) \sin(k_3z). \tag{4c}$$

Here $k_3 = p\pi/d$, $p = 1,2,3,\cdots$, and

$$k_2^2 + k_3^2 = \mu_e k_o^2, \tag{5}$$

$$\alpha_2 = k_2/\sqrt{\mu_e}\, k_o \quad , \alpha_3 = k_3/\sqrt{\mu_e}\, k_o. \tag{6}$$

Dispersion relations between k_2 and ω can be uniquely determined via Eqs.(5) and (1). We note that, since μ_e can be varied by varying ω_o, dispersion relations derived for the present case are subject to frequency tuning. This is contrasted to the general case to be considered next that dispersion relations are specified under fixed magnetic field biasing conditions.

(3) General case

If $\alpha_1 \neq 0$, the two modes, (±), will form coupled modes in order to satisfy the metal boundary conditions at z = 0 and d. Denote (α_1, α_2, α_3) as the directional cosines for the (+) mode and (β_1, β_2, β_3) the directional cosines for the (-) mode. Similar to the phenomenon of birefringence, the condition for coupling requires matched phases of the two modes on the boundaries. This implies

$$\sqrt{\mu_e^{(+)}}\, \alpha_1 = \sqrt{\mu_e^{(-)}}\, \beta_1 \ , \quad \sqrt{\mu_e^{(+)}}\, \alpha_2 = \sqrt{\mu_e^{(-)}}\, \beta_2 \ . \tag{7}$$

For guiding modes the (±) modes form standing waves in the z direction. Denote p and p′ as the orders of the standing waves for the (+) and (-) modes, respectively. We note that p and p′ are nonzero positive integers which are necessarily unequal (since $\mu_e^{(+)} \neq \mu_e^{(-)}$). Therefore,

$$\alpha_3 = p\pi/dk_o, \ \beta_3 = p'\pi/dk_o \tag{8}$$

subject to the following constraints

$$\alpha_1^2 + \alpha_2^2 + \alpha_3^2 = 1, \ \beta_1^2 + \beta_2^2 + \beta_3^2 = 1. \tag{9}$$

Eqs.(8) and (9) together with Eq.(A5) solve uniquely the dispersion relations for the coupled modes. We note that for given values of k_1 and k_2, a propagating mode can be found at a frequency ω only if ω_o is specified at

some discrete values (depending on the values of p and p'). No frequency tuning is allowed for the present coupled-mode solutions. Nevertheless, both coupled and uncoupled modes are reciprocal guiding modes.

Let us now derive the field profiles of the coupled modes. The coupled modes are composed of four plane waves with directional cosines $(\alpha_1, \alpha_2, \alpha_3)$, $(\beta_1, \beta_2, \beta_3)$, $(\beta_1, \beta_2, -\beta_3)$, $(\alpha_1, \alpha_2, -\alpha_3)$ whose relative amplitudes are denoted as 1, X, Y, and Z, respectively. The three unknowns X, Y, and Z shall be determined via the boundary conditions at z = 0 which require e_x, e_y, and b_z to vanish (boundary conditions at z = d are automatically satisfied in view of Eq.(8)). Therefore,

$$\tilde{b}_z(\alpha_1,\alpha_2,\alpha_3) + X\tilde{b}_z(\beta_1,\beta_2,\beta_3) + Y\tilde{b}_z(\beta_1,\beta_2,-\beta_3) + Z\tilde{b}_z(\alpha_1,\alpha_2,-\alpha_3) = 0, \quad (10a)$$

$$\tilde{e}_x(\alpha_1,\alpha_2,\alpha_3) + X\tilde{e}_x(\beta_1,\beta_2,\beta_3) + Y\tilde{e}_x(\beta_1,\beta_2,-\beta_3) + Z\tilde{e}_x(\alpha_1,\alpha_2,-\alpha_3) = 0, \quad (10b)$$

$$\tilde{e}_y(\alpha_1,\alpha_2,\alpha_3) + X\tilde{e}_y(\beta_1,\beta_2,\beta_3) + Y\tilde{e}_y(\beta_1,\beta_2,-\beta_3) + Z\tilde{e}_y(\alpha_1,\alpha_2,-\alpha_3) = 0. \quad (10c)$$

Special features concerning X, Y, and Z may be deduced by observing the following. Since, from Eqs.(A2a), (A2b), and (A4c), one finds

$$\tilde{b}_z(\alpha_1,\alpha_2,\alpha_3) = -\tilde{b}_z(\alpha_1,\alpha_2,-\alpha_3)^*, \quad (11a)$$

$$\tilde{e}_x(\alpha_1,\alpha_2,\alpha_3) = -\tilde{e}_x(\alpha_1,\alpha_2,-\alpha_3)^*, \quad (11b)$$

$$\tilde{e}_y(\alpha_1,\alpha_2,\alpha_3) = -\tilde{e}_y(\alpha_1,\alpha_2,-\alpha_3)^*, \quad (11c)$$

it can be proved that solutions to Eqs.(10a) to (10c) shall satisfy the following relationships in general

$$ZZ^* = 1, \quad XYZ^* - X^*Y^*Z = 0. \quad (12)$$

This enables us to define new coefficients for the constituent waves which possess more symmetry. Let us multiply the four coefficients (1, X, Y, Z) by $Z^{-1/2}$ and define two new parameters A and B as follows

$$A = Z^{-1/2}, \quad B = XZ^{-1/2}. \quad (13)$$

The relative proportions of the four waves $(\alpha_1,\alpha_2,\alpha_3)$, $(\alpha_1,\alpha_2,-\alpha_3)$,

$(\beta_1,\beta_2,\beta_3)$, and $(\beta_1,\beta_2,-\beta_3)$ become now A, A^*, B, and B^*, respectively. Usage of A and B can largely simplify the field expressions for coupled modes which can be written as follows

$$e_x = j\exp(-jk_1x-jk_2y)\{\mathrm{Im}[A\tilde{e}_x(\alpha)\exp(-jk_o\alpha_3z)] + \mathrm{Im}[B\tilde{e}_x(\beta)\exp(-jk_o\beta_3z)]\}, \quad (14a)$$

$$e_y = j\exp(-jk_1x-jk_2y)\{\mathrm{Im}[A\tilde{e}_y(\alpha)\exp(-jk_o\alpha_3z)] + \mathrm{Im}[B\tilde{e}_y(\beta)\exp(-jk_o\beta_3z)]\}, \quad (14b)$$

$$e_z = \exp(-jk_1x-jk_2y)\{\mathrm{Re}[A\exp(-jk_o\alpha_3z)]\tilde{e}_z(\alpha) + \mathrm{Re}[B\exp(-jk_o\beta_3z)]\tilde{e}_z(\beta)\}, \quad (14c)$$

$$h_x = \exp(-jk_1x-jk_2y)\{\mathrm{Re}[A\tilde{h}_x(\alpha)\exp(-jk_o\alpha_3z)] + \mathrm{Re}[B\tilde{h}_x(\beta)\exp(-jk_o\beta_3z)]\}, \quad (15a)$$

$$h_y = \exp(-jk_1x-jk_2y)\{\mathrm{Re}[A\tilde{h}_y(\alpha)\exp(-jk_o\alpha_3z)] + \mathrm{Re}[B\tilde{h}_y(\beta)\exp(-jk_o\beta_3z)]\}, \quad (15b)$$

$$h_z = j\exp(-jk_1x-jk_2y)\{\mathrm{Im}[A\tilde{h}_z(\alpha)\exp(-jk_o\alpha_3z)] + \mathrm{Im}[B\tilde{h}_z(\beta)\exp(-jk_o\beta_3z)]\}, \quad (15c)$$

$$b_x = h_x, \quad (16a)$$

$$b_y = \exp(-jk_1x-jk_2y)\{\mathrm{Re}[A\tilde{b}_y(\alpha)\exp(-jk_o\alpha_3z)] + \mathrm{Re}[B\tilde{h}_y(\beta)\exp(-jk_o\beta_3z)]\}, \quad (16b)$$

$$b_z = j\exp(-jk_1x-jk_2y)\{\mathrm{Im}[A\tilde{b}_z(\alpha)\exp(-jk_o\alpha_3z)] + \mathrm{Im}[B\tilde{b}_z(\beta)\exp(-jk_o\beta_3z)]\}, \quad (16c)$$

where $\tilde{e}_x(\alpha)$ abbreviates for $\tilde{e}_x(\alpha_1,\alpha_2,\alpha_3)$, for example. We note that while solutions to uncoupled modes shown in Eqs.(2a) to (4c) are of the TE type, the coupled modes, Eqs.(14a) to (16c), are neither TE nor TM modes, since e_z and h_z are normally nonvanishing in general. They are denoted as EM modes.

II. Resonatant modes in ferrite patch antenna

Let the patch possess rectangular geometry with length a and width b parallel to x and y directions, respectively. The guiding waves derived above for parallel plate waveguide become quantized in the lateral directions. Specifically, we write

$$k_x = m\pi/a,\ m = 0,\ 1,\ 2,\ \cdots,\ \text{for coupled modes},$$
$$= 0,\ \text{for uncoupled modes}, \quad (17a)$$

$$k_y = n\pi/b,\ n = 0,\ 1,\ 2,\ \cdots,\ \text{for coupled and uncoupled modes}. \quad (17b)$$

Note that m can take only value of 0 in the uncoupled mode case, since the Voigt configuration restrict the field to have no variations along the dc field direction, the x-axis. Resonant frequencies can be deduced by using the above k_x and k_y values in Eqs.(5) and (1) for uncoupled modes and Eqs.(A5) and (7) to (9) for coupled modes, provided that the solutions satisfy confinement or insulating boundary conditions at the patch antenna periphery as discussed in the preceding section. Coupled modes and uncoupled modes will be separately discussed in the following.

(1) TE_{0np} modes

From Eqs.(2a) to (4c) one may construct the following field profiles for the Voigt configuration

$$e_x = E_o \sin(k_2 y) \sin(k_3 z), \tag{18a}$$

$$e_y = 0, \tag{18b}$$

$$e_z = 0, \tag{18c}$$

$$h_x = 0, \tag{19a}$$

$$h_y = \frac{E_o}{j\zeta}\left\{\exp(-jk_2 y)\ \mathrm{Re}\left[\frac{\alpha_2\alpha_3\mu_e\omega j + (1 - \alpha_2{}^2\mu_e)\omega_o + \omega_m}{(\omega_o + \omega_m)\alpha_3 + \alpha_2\omega j}\exp(-jk_3 z)\right]\right.$$

$$\left. + \exp(jk_2 y)\ \mathrm{Re}\left[\frac{\alpha_2\alpha_3\mu_e\omega j - (1 - \alpha_2{}^2\mu_e)\omega_o - \omega_m}{(\omega_o + \omega_m)\alpha_3 - \alpha_2\omega j}\exp(-jk_3 z)\right]\right\}, \tag{19b}$$

$$h_z = \frac{E_o}{j\zeta}\left\{\exp(-jk_2 y)\ \mathrm{Im}\left[\frac{-(1 - \alpha_3{}^2\mu_e)\omega j - \alpha_2\alpha_3\mu_e\omega_o}{(\omega_o + \omega_m)\alpha_3 + \alpha_2\omega j}\exp(-jk_3 z)\right]\right.$$

$$\left. - \exp(jk_2 y)\ \mathrm{Im}\left[\frac{-(1 - \alpha_3{}^2\mu_e)\omega j + \alpha_2\alpha_3\mu_e\omega_o}{(\omega_o + \omega_m)\alpha_3 - \alpha_2\omega j}\exp(-jk_3 z)\right]\right\}, \tag{19c}$$

$$b_x = 0, \tag{20a}$$

$$b_y = \frac{\alpha_3 \mu_o \mu_e E_o}{j\,\zeta} \sin(k_2 y)\, \cos(k_3 z), \tag{20b}$$

$$b_z = \frac{-\alpha_2 \mu_o \mu_e E_o}{j\,\zeta} \cos(k_2 y)\, \sin(k_3 z). \tag{20c}$$

The above solutions do not satisfy magnetic wall boundary conditions at the cavity periphery. However, one may readily show that $\vec{e} \times \vec{h} \cdot \hat{n}$ vanishes at all points of the periphery and hence energy is confined to the interior of the cavity. Here $\hat{n}$ denotes the unit vector normal to the wall periphery. The above solutions are termed transverse TE modes denoted as TE_{0np}. Radiation frequencies of TE_{0np} modes may be tuned via changing the dc biasing field. Radiations may be visualized as arising from the equivalent currents distributed on the insulating wall. Since only h_z is nonvanishing on the wall, radiations are due to electric currents induced by h_z through Ampere law. Since h_z averages to zero on the side walls $x = 0$ and $x = a$, radiations are mainly resulted from electric currents along the dc field direction on the side walls $y = 0$ and $y = b$.

(2) $TE_{m0p/p'}$ modes

One may superpose the coupled mode solutions, Eqs.(14a) to (16c), to form the following solutions

$$e_x = j\cos(k_1 x)\Big\{\exp(-jk_2 y)\left[\mathrm{Im}[A\tilde{e}_x(\alpha)\exp(-jk_o\alpha_3 z)] + \mathrm{Im}[B\tilde{e}_x(\beta)\exp(-jk_o\beta_3 z)]\right] - \exp(jk_2 y)\left[\mathrm{Im}[A\tilde{e}_x^{*}(\alpha)\exp(-jk_o\alpha_3 z)] + \mathrm{Im}[B\tilde{e}_x^{*}(\beta)\exp(-jk_o\beta_3 z)]\right]\Big\}, \tag{21a}$$

$$e_y = -\sin(k_1 x)\Big\{\exp(-jk_2 y)\left[\mathrm{Im}[A\tilde{e}_y(\alpha)\exp(-jk_o\alpha_3 z)] + \mathrm{Im}[B\tilde{e}_y(\beta)\exp(-jk_o\beta_3 z)]\right] + \exp(jk_2 y)\left[\mathrm{Im}[A\tilde{e}_y^{*}(\alpha)\exp(-jk_o\alpha_3 z)] + \mathrm{Im}[B\tilde{e}_y^{*}(\beta)\exp(-jk_o\beta_3 z)]\right]\Big\}, \tag{21b}$$

$$e_z = -2\sin(k_1 x)\sin(k_2 y)\left[\mathrm{Re}[A\exp(-jk_o\alpha_3 z)]\tilde{e}_z(\alpha)+\mathrm{Re}[B\exp(-jk_o\beta_3 z)]\tilde{e}_z(\beta)\right], \tag{21c}$$

$$h_x = j\sin(k_1x)\{\exp(-jk_2y)[\mathrm{Re}[A\tilde{h}_x(\alpha)\exp(-jk_o\alpha_3z)] + \mathrm{Re}[B\tilde{h}_x(\beta)\exp(-jk_o\beta_3z)]] + \exp(jk_2y)[\mathrm{Re}[A\tilde{h}_x^*(\alpha)\exp(-jk_o\alpha_3z)] + \mathrm{Re}[B\tilde{h}_x^*(\beta)\exp(-jk_o\beta_3z)]]\}, \quad (22a)$$

$$h_y = \cos(k_1x)\{\exp(-jk_2y)[\mathrm{Re}[A\tilde{h}_y(\alpha)\exp(-jk_o\alpha_3z)] + \mathrm{Re}[B\tilde{h}_y(\beta)\exp(-jk_o\beta_3z)]] - \exp(jk_2y)[\mathrm{Re}[A\tilde{h}_y^*(\alpha)\exp(-jk_o\alpha_3z)] + \mathrm{Re}[B\tilde{h}_y^*(\beta)\exp(-jk_o\beta_3z)]]\}, \quad (22b)$$

$$h_z = j\cos(k_1x)\{\exp(-jk_2y)[\mathrm{Im}[A\tilde{h}_z(\alpha)\exp(-jk_o\alpha_3z)] + \mathrm{Im}[B\tilde{h}_z(\beta)\exp(-jk_o\beta_3z)]] + \exp(jk_2y)[\mathrm{Im}[A\tilde{h}_z^*(\alpha)\exp(-jk_o\alpha_3z)] + \mathrm{Im}[B\tilde{h}_z^*(\beta)\exp(-jk_o\beta_3z)]]\}, \quad (22c)$$

$$b_x = h_x, \quad (23a)$$

$$b_y = \cos(k_1x)\{\exp(-jk_2y)[\mathrm{Re}[A\tilde{b}_y(\alpha)\exp(-jk_o\alpha_3z)] + \mathrm{Re}[B\tilde{b}_y(\beta)\exp(-jk_o\beta_3z)]] - \exp(jk_2y)[\mathrm{Re}[A\tilde{b}_y^*(\alpha)\exp(-jk_o\alpha_3z)] + \mathrm{Re}[B\tilde{b}_y^*(\beta)\exp(-jk_o\beta_3z)]]\}, \quad (23b)$$

$$b_z = j\cos(k_1x)\{\exp(-jk_2y)[\mathrm{Im}[A\tilde{b}_z(\alpha)\exp(-jk_o\alpha_3z)] + \mathrm{Im}[B\tilde{b}_z(\beta)\exp(-jk_o\beta_3z)]] + \exp(jk_2y)[\mathrm{Im}[A\tilde{b}_z^*(\alpha)\exp(-jk_o\alpha_3z)] + \mathrm{Im}[B\tilde{b}_z^*(\beta)\exp(-jk_o\beta_3z)]]\}, \quad (23c)$$

The above solutions are denoted as $EM_{mnp/p'}$ modes, since they are neither TE nor TM modes. It is noted that these modes, again, do not satisfy magnetic wall boundary conditions at the cavity periphery. One may evaluate the quantity $\vec{e} \times \vec{h} \cdot \hat{n}$ on the cavity periphery and find that insulating wall boundary conditions can be rigorously satisfied only for the n = 0 modes (this is because that e_x vanishes at y = 0 and y = d planes only if n = 0). Therefore, the n = 0 modes are normal modes of the cavity, whereas the $n \neq 0$ modes are leaky modes of the cavity. However, from Eq.(21c), one finds that for n = 0 modes e_z vanishes identically in the cavity. This implies that n =

0 modes are actually TE modes. These modes are termed longitudinal TE modes denoted as $TE_{m0p/p'}$, since they do not vary along the y direction (perpendicualr to the dc field direction). From Eq.(22c) one finds that h_z averages to zero on the side walls y = 0 and y = b. Therefore, radiation from a longitudinal TE modes is due to the equivalent currents induced by h_z along the y direction on the x = 0 and x = a side walls. Therefore, the polarization of the radiated field from a longitudinal TE mode is perpendicular to that from a transverse TE mode, and, hence the two modes may be visualized as complementary to each other. However, longitudinal TE modes are discrete modes in the frequency domain, which are subject to no frequency tuning capability via the applied dc magnetic field.

Calculational Results

In this section normalized units are used for the purpose of general discussions. The normalized frequencies are defined as $f = \omega/\omega_m$, and $f_o = \omega_o/\omega_m$ and all of the distances have been normalized with respect to $(2\pi\omega_m)^{-1}(\epsilon\mu_o)^{-1/2}$. The ferrite patch is considered of square geometry with a = b = 3. Fig.1 shows the resonant frequencies of the normal modes of a ferrite patch antenna, TE_{0np} and $TE_{m0p/p'}$. In this drawing d = 0.03. It is seen that the transverse TE modes form continuous spectra whose values can be tuned via the biasing field over a wide frequency range ($\geq$ 100 %). This is contrasted to the longitudinal TE modes which are discrete modes existing only at fixed values of the biasing field (shown as little spots in Fig. 1). In Ref.5 it was reported that 40% frequency tunability was measured for a rectangular ferrite patch antenna which was biased by an in-plane magnetic field. This is consistent with our transverse TE mode calculations. Furthermore, since a transverse TE mode may be tuned to the same frequency

as the longitudinal one, circularly polarized radiations may be possible in the frequency range where the longitudinal TE mode is operational. It was reported in Ref.5 that cross polarization was measured for a ferrite patch antenna whose intensity was 10 dB below the main beam radiation. Circularly polarized radiations were also measured in another laboratory[11] for a ferrite patch antenna whose two polarizaton components were subject to different frequency tuning capabilities. For one polarization direction the frequency can be continuously tuned over a wide frequency range, whereas for the other polarization direction the radiation was almost fixed to a certain biasing field value. This is totally consistent with our model calculations reported here.

Table 1 depicts the values of modal frequency f, normalized biasing field f_o, and $\mu_e^{(+)}$ for the $EM_{mnp/p'}$ modes for the same patch antenna described in Fig.1. In table 1 it is found that f_o is smaller than f. For different m and n values the differences in f and f_o are small, since a >> d. $\mu_e^{(+)}$ presumes very different values if p or p' values are different. We note that only n = 0 modes can be normal modes of the cavity. Fig.2 shows the modal frequencies of the coupled modes $EM_{mnp/p'}$, p' = 1, 2 and 3, as a function of the ferrite substrate thickness d. The modal frequencies of these modes increase with decreasing values of d, as one may expect from a normal cavity resonator. Fig.3 shows the net energy flow across the ferrite cavity periphery as a function of d. The energy flow is defined as surface integration of the quantity $\vec{e} \times \vec{h} \cdot \hat{n}$ over the cavity periphery. It is seen that energy flow decreases with decreasing d. It decreases with decreasing value of n and vanishes identically only if n = 0. Therefore, only n = 0 modes can form normal modes of the cavity, denoted as $TE_{m0p/p'}$, and n ≠ 0

modes are leaky modes of the cavity.

Measurements

We have fabricated a square patch antenna using magnesium-ferrite substrate, TT1-1000 (Trans-Tech, MD). The substrate is of dimension 0.02" × 2" × 2", and the patch is 3/8" × 3/8". A microstrip line of width 0.43 mm is fed into the antenna at the center of one side of the patch. The antenna was inserted in an electromagnet which provided magnetic fields up to 9 kOe. The magnetic field was applied along the edge of one side of the patch and perpendicular to the microstrip feed line. S_{11} data were taken using a network analyzer (HP8510B) which was connected to an HP computer. Fig.4 shows the measured resonant frequencies of the patch antenna as a function of the applied magnetic field.

In Fig.4 full dots represent biasing-below-FMR data, and open dots above FMR. The dashed lines are purely dielectric or uncoupled modes whose frequencies are independent of the applied field. The intensities as measured in changes in S_{11} of the dielectric or uncoupled modes were very weak compared to the ferrite or coupled modes. The uncoupled modes were observed mostly for magnetic fields below FMR. The solid lines in Fig.4 are theoretical curves for the Voigt modes converted from Fig.1 using the following parameters: $4\pi M_s$ = 985 G, ϵ = 11.41, and a = 0.91 cm. The $4\pi M_s$ and ϵ values are furnished by the manufacturer, and the patch dimension, a, is determined by a best-fit algorithm, since the physical dimension of the patch does not imply the dimension of the embedded cavity resonator. A discrete data point, solid diamond, is also shown in the near-FMR region of Fig.4 reminicent of the longitudinal TE mode. Since the longitudinal TE mode

exhibited very low intensity, other higher-order longitudinal TE modes were not observed in the present S_{11} measurements. When comparing Fig.4 with Fig.1 one notices the good agreement between the theory and the experiments.

Conclusions

We have calculated the normal modes of radiations from rectangular patch antennas loaded with ferrite materials. Two kinds of normal modes are found. The transverse TE modes can be tuned over a wide frequency range via the applied biasing magnetic field, whereas the longitudinal TE modes are discrete modes and fixed in the frequency domain. Since the polarizations of the radiation patterns for the two kinds of modes are spatially perpendicular to each other, circularly polarized radiations may be obtained for frequencies at which longitudinal TE modes are excited. The theory compared very well with experiments.

Appendix

The bulk modes, which are used as the building blocks for the resonant modes of a ferrite patch antenna, are summarized in this Appendix.[10]

$$\tilde{h}_x = \alpha_1\mu_e\{\alpha_3\omega j - \alpha_2[\omega_o + \omega_m/(1 - \mu_e)]\}, \tag{A1a}$$

$$\tilde{h}_y = \alpha_2\alpha_3\mu_e\omega j + (1 - \alpha_2{}^2\mu_e)\omega_o + [1 + \alpha_1{}^2\mu_e/(1-\mu_e)]\omega_m, \tag{A1b}$$

$$\tilde{h}_z = -(1 - \alpha_3{}^2\mu_e)\omega j - \alpha_2\alpha_3\mu_e\omega_o, \tag{A1c}$$

$$\tilde{e}_x = \zeta\{\alpha_3\omega_o + \alpha_2\omega j + \alpha_3\omega_m[1 + \alpha_1{}^2\mu_e/(1-\mu_e)]\}, \tag{A2a}$$

$$\tilde{e}_y = -\zeta\alpha_1[\omega j - \alpha_2\alpha_3\mu_e\omega_m/(1-\mu_e)], \tag{A2b}$$

$$\tilde{e}_z = -\zeta\alpha_1[\omega_o + (1 - \alpha_3{}^2\mu_e)\omega_m/(1-\mu_e)], \tag{A2c}$$

$$\tilde{m}_x = 0, \tag{A3a}$$

$$\tilde{m}_y = -(1 - \mu_e)\omega_o - (1 - \alpha_3{}^2\mu_e)\omega_m, \tag{A3b}$$

$$\tilde{m}_z = (1 - \mu_e)\omega j - \alpha_2\alpha_3\mu_e\omega_m, \tag{A3c}$$

$$\tilde{b}_x = \mu_o h_x, \tag{A4a}$$

$$\tilde{b}_y = \mu_o\mu_e\{\alpha_2\alpha_3\omega j + (1 - \alpha_2^2)\omega_o + [\alpha_1^2/(1-\mu_e) + \alpha_3^2]\omega_m\}, \tag{A4b}$$

$$\tilde{b}_z = -\mu_o\mu_e[(1 - \alpha_3^2)\omega j + \alpha_2\alpha_3(\omega_o + \omega_m)], \tag{A4c}$$

where ζ is given by $\zeta = \sqrt{\mu_o/\epsilon}$. The dispersion relation can be expressed in terms of an effective permeability value μ_e given by

$$\mu_e = k^2/k_o^2$$

$$= 1 + \frac{2\alpha_1^2\omega_m}{(1+\alpha_1^2)\omega_o + (1-\alpha_1^2)\omega_m \mp \left[(1-\alpha_1^2)^2(\omega_o+\omega_m)^2 + 4\alpha_1^2\omega^2\right]^{1/2}}, \tag{A5}$$

where α_1 denotes the directional cosine of $\vec{k}$ with respect to x-axis, etc., and ω_o and ω_m are defined as

$$\omega_o = -\gamma\mu_o H_{in}, \quad \omega_m = -\gamma\mu_o M_s. \tag{A6}$$

Here γ is the gyromagnetic ratio, M_s is the saturation magnetization, and H_{in} denotes the internal dc magnetic field.

References

1. D. Polder, "On the theory of electromagnetic resonance", Phil. Mag. 40, 99 (1949).
2. H. Suhl, and L. R. Walker, "Faraday rotation of guided waves", Phys. Rev. **86**, 122 (1952).
3. H. Unz, "Propagation in arbitrarily magnetized ferrites between two conducting parallel planes", IEEE Trans. MTT-11, 204 (1963).
4. N. Okamoto and S. Iketa, "An experimental study of electronic scaning by an antenna loaded with a circular array of ferrite rods", IEEE Trans. AP-27, 426, 1979.
5. D. M. Pozar and V. Scanchez, "Magnetic tuning of a microstrip antenna on a ferrite substrate", Elect. Lett. 24(12), 729, 1988.

6. L.C. Shen, "The elliptical microstip antenna with circular polarization", IEEE Trans. **AP-29**, 90, 1981.

7. A.G. Derneryd, "A theoretical investigation of the rectangular microstrip antenna element", IEEE Trans. **AP-26**, 532, 1978.

8. Y.T. Lo D. Solomon, and W.F. Richards, "Theory and experiment on microstrip antennas", IEEE Trans. **MTT-27**, 137, 1979.

9. H. How and C. Vittoria, "Ferrite disc antennas: a dual-frequency radiator design", to be published.

10. B. L. Lax and K. J. Button, "Microwave ferrites and ferrimagnetics", McGraw-Hill, 1962, New York.

11. Private communication with M. Champion and P. Ranville of Hanscom AFB, MA.

Table Caption

Table 1 Modal frequency f, biasing field fo, and $\mu_e^{(+)}$ for various coupled modes, $EM_{mnp/p'}$. The ferrite substrate thickness d is equal to 0.03.

Figure Captions

Fig.1 Mode chart for a square ferrite patch antenna, a = b = 3, d = 0.03.

Fig.2 Modal frequency f of the EM modes as a function of the ferrite substrate thickness d.

Fig.3 Net energy flow across the cavity periphery as a function of the ferrite substrate thickness d.

Fig.4 Measured resonant frequencies of a square ferrite patch antenna.

m	n	p	p′	f	f_o	$\mu_e^{(+)}$	type
1	0	2	1	16.66745	16.34748	3.99972	normal
1	0	3	1	16.66745	16.23945	8.99925	normal
1	1	2	1	16.66829	16.34833	3.99942	leaky
1	1	3	1	16.66828	16.24029	8.99845	leaky
1	2	2	1	16.67078	16.35088	3.99852	leaky
1	2	3	1	16.67078	16.24281	8.99605	leaky
2	2	2	1	16.67314	16.35333	3.99769	leaky
2	2	3	1	16.67314	16.24519	8.99381	leaky
1	0	1	2	33.33374	32.16745	0.25002	normal
1	0	3	2	33.33374	33.24590	2.24997	normal
1	0	1	3	50.00027	48.93780	0.11112	normal
1	0	2	3	50.00027	48.60185	0.44445	normal

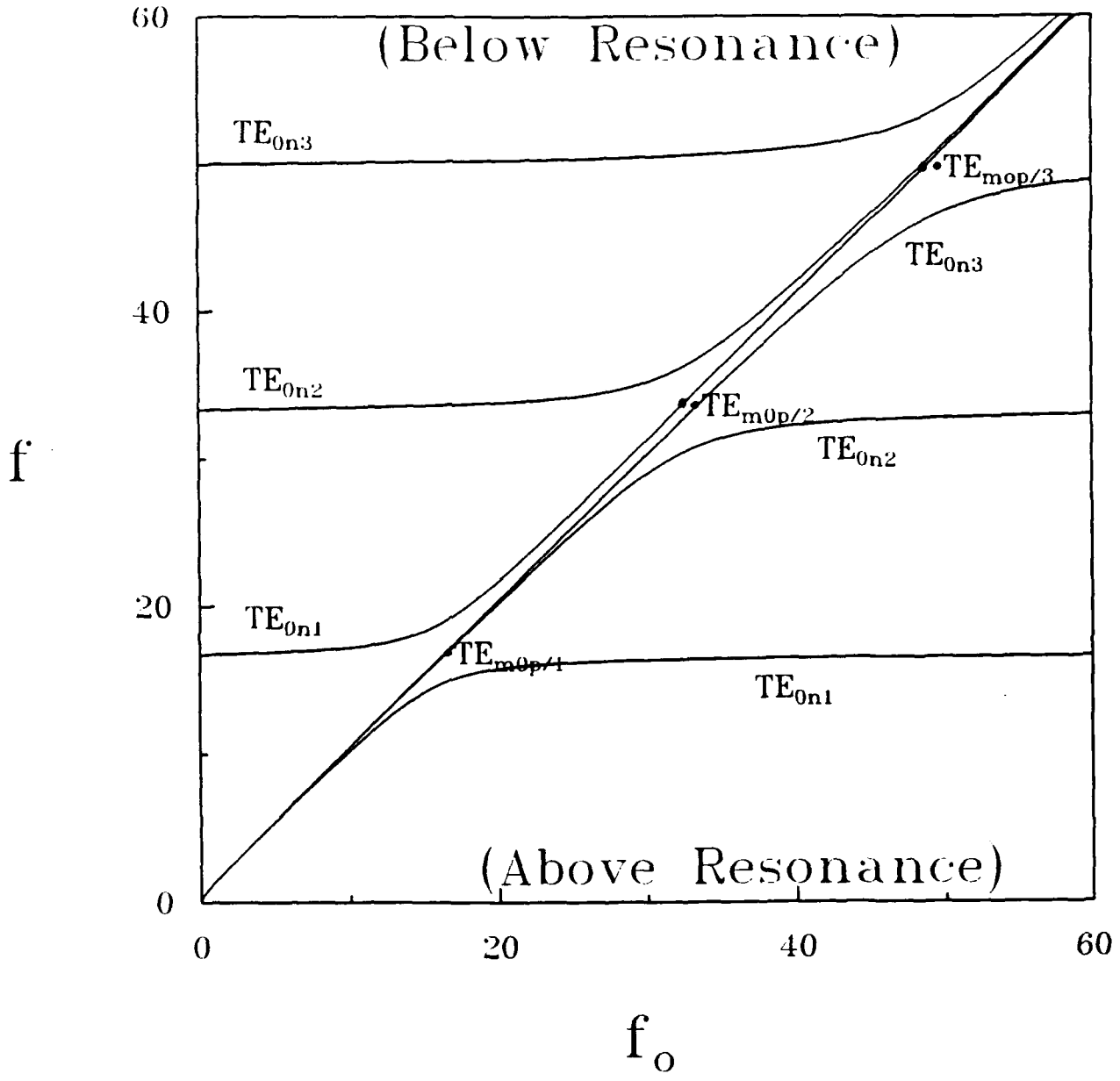
(Below Resonance)
TE_{0n3}
$TE_{mop/3}$
TE_{0n3}
TE_{0n2}
$TE_{m0p/2}$
TE_{0n2}
TE_{0n1}
$TE_{m0p/1}$
TE_{0n1}
(Above Resonance)
60
40
20
0
0
20
40
60
f
f_o

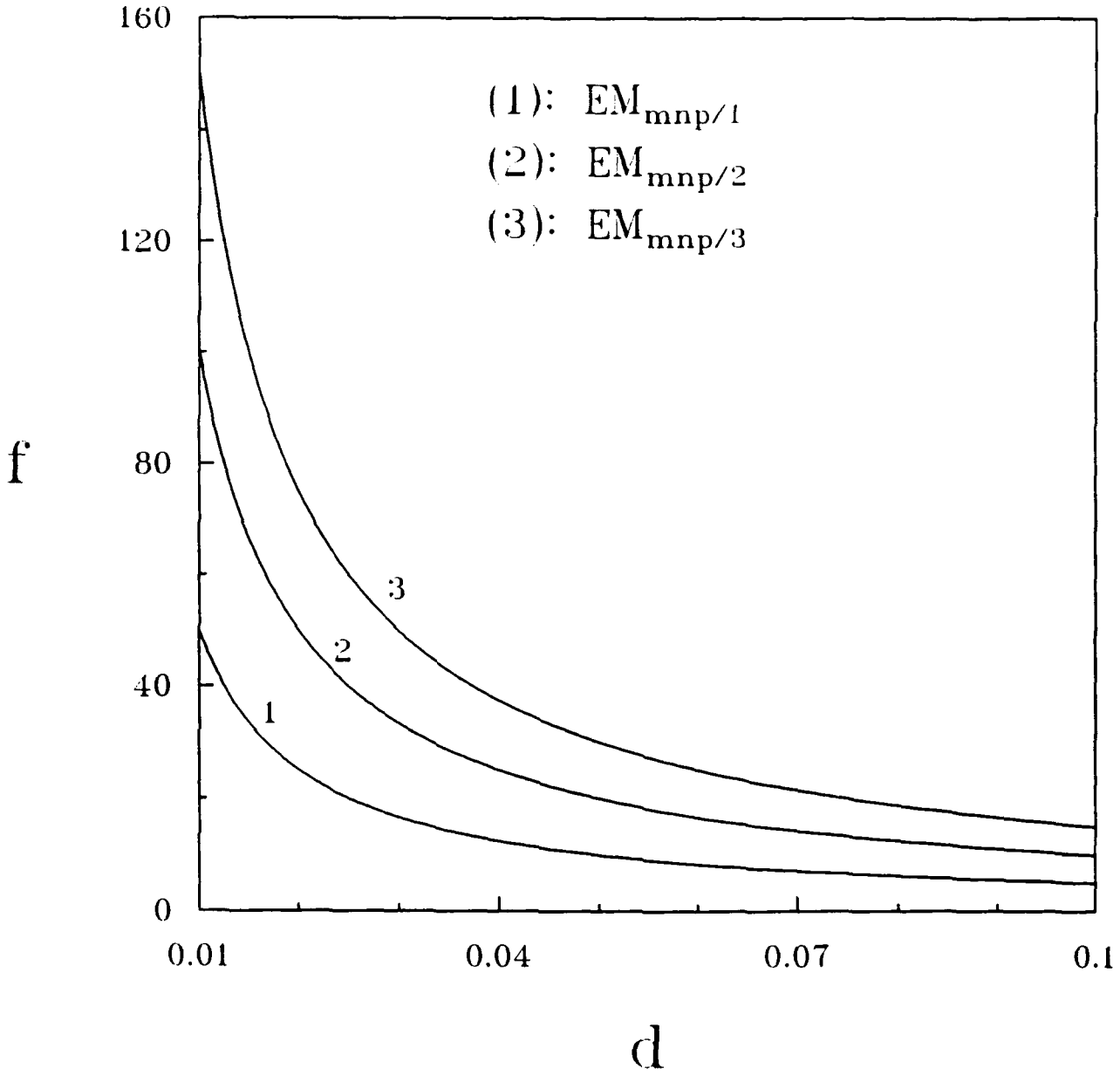
160
120
80
40
0
f
0.01
0.04
0.07
0.1
d
(1): EM mnp/1
(2): EM mnp/2
(3): EM mnp/3
1
2
3

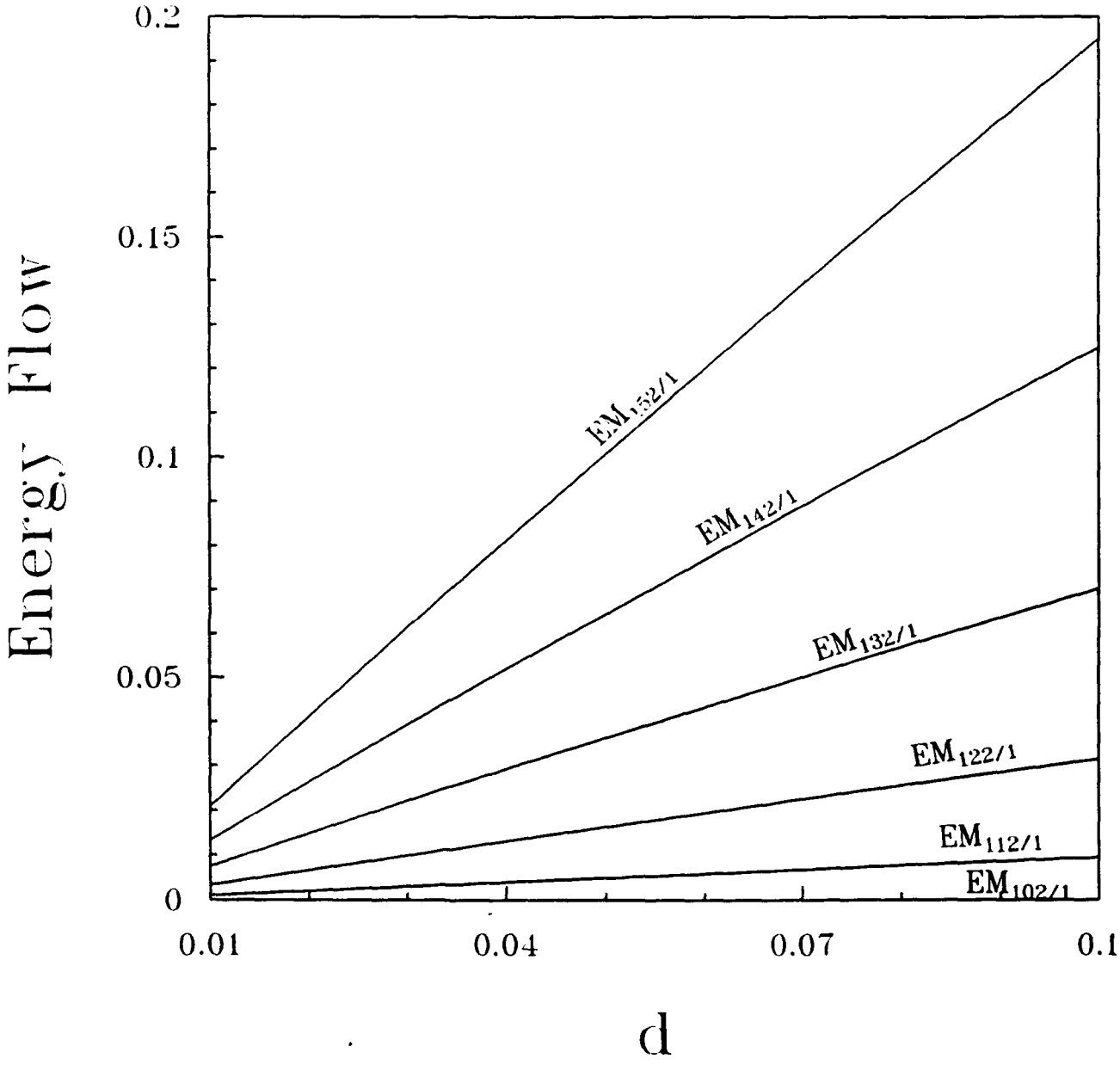
Energy Flow
0.2
0.15
0.1
0.05
0
0.01
0.04
0.07
0.1
d
EM132/1
EM142/1
EM132/1
EM122/1
EM112/1
EM102/1

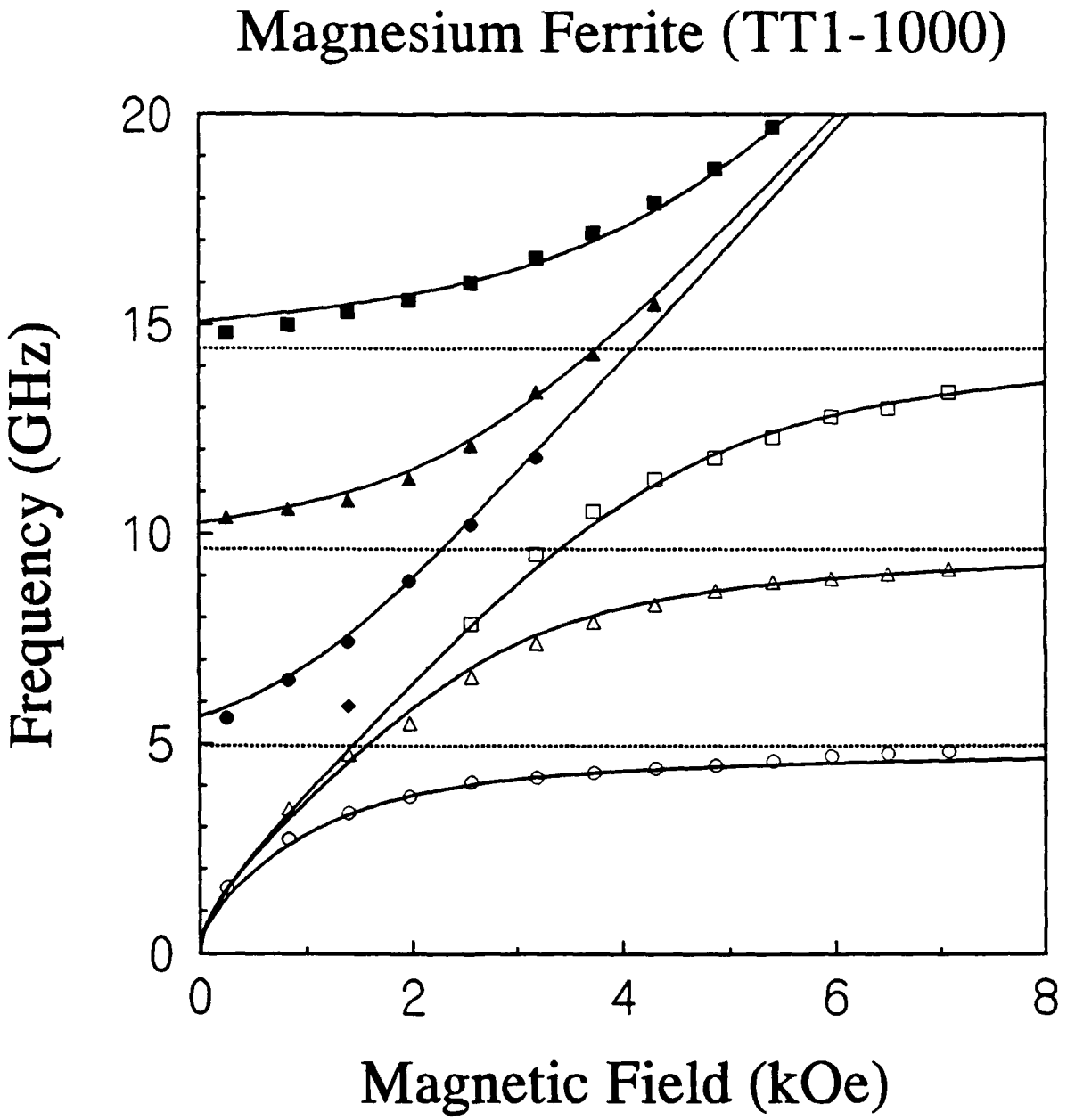

$4\pi M_s$ = 985 G, ε = 11.41, a = 0.91 cm